Al and Zn phenoxy-amidine complexes for lactide ROP catalysis

Benjamin Théron, Valentin Vaillant-Coindard, Cédric Balan, Yoann Rousselin, Jérôme Bayardon, Raluca Malacea-Kabbara, Pierre Le Gendre

▶ **To cite this version:**

Benjamin Théron, Valentin Vaillant-Coindard, Cédric Balan, Yoann Rousselin, Jérôme Bayardon, et al.. Al and Zn phenoxy-amidine complexes for lactide ROP catalysis. Dalton Transactions, 2023, 52 (23), pp.7854-7868. 10.1039/D3DT01216F . hal-04225864

HAL Id: hal-04225864
https://hal.science/hal-04225864

Submitted on 3 Oct 2023

HAL is a multi-disciplinary open access archive for the deposit and dissemination of scientific research documents, whether they are published or not. The documents may come from teaching and research institutions in France or abroad, or from public or private research centers.

L'archive ouverte pluridisciplinaire **HAL**, est destinée au dépôt et à la diffusion de documents scientifiques de niveau recherche, publiés ou non, émanant des établissements d'enseignement et de recherche français ou étrangers, des laboratoires publics ou privés.

Al and Zn phenoxy-amidine complexes for lactide ROP catalysis

Benjamin Théron,†[a] Valentin Vaillant-Coindard,†[a] Cédric Balan,[a] Yoann Rousselin,[a] Jérôme Bayardon,[a] Raluca Malacea Kabbara[a] and Pierre Le Gendre*[a]

We report the synthesis of a new generation of phenoxy-amidine ligands based on an aryloxy moiety possessing an *ortho*-*N*-linked trisubstituted amidine. The reaction of the phenol-amidine proligands with aluminum and zinc alkyls gave mono- or bis-ligated complexes depending on the metal/ligand ratio used. The solid-state structure of four proligands and thirteen Zn and Al complexes has been determined by X-Ray diffraction analysis. The mono-ligated complexes present an aryloxy-bridged dimeric structure, which is retained in solution in the case of Zn complexes but not with aluminum according to DOSY NMR experiments. Bis(ligated) Al and Zn complexes exhibit fluxional behaviour in solution attributed to coordination-decoordination of the amidine moiety and the rotation around the amidine C-NR'$_2$ and C-Ar bonds. These complexes were tested for the ROP of *rac*-lactide in solution and under bulk conditions. In both cases, the most performant catalysts are Zn complexes featuring a phenoxy-amidine ligand with a pendant additional dimethylamino arm.

Introduction

Phenoxy-imines (often abbreviated as FI) are among the most versatile ligands in coordination chemistry[1] and their complexes have found applications in many fields ranging from catalysis[2] to pharmacology,[3] molecular magnets,[4] or sensors.[5] Their ease of access and modularity allow to fine-tune the properties of the corresponding complexes according to the targeted application and thus to access very efficient systems. A more drastic modification of the FI ligand skeleton by replacing either the imine or the phenoxy group by another moiety has also led to extremely efficient systems,[6] sometimes even more efficient than the parent FI complexes. In this context, we have recently described a new variant of FI ligands that are phenoxy-amidines (FA type **A**, Fig. 1) and demonstrated their coordination ability.[7] One drawback, however, of **A** ligands is that the amidine function in the proligands (i.e. phenol-amidine **AH**) has a *trans* configuration that is not suitable for metal chelation, but it isomerizes upon coordination with the metal. This isomerization is slightly penalizing at the thermodynamic level and can lead to a more complicated coordination chemistry than expected. To address this problem, we have designed a phenoxy-amidine ligands (**B**) where the amidine function is oriented differently by being grafted through the nitrogen *via* a methylene spacer to the aryloxy unit.[8] We have shown that these ligands can form chelate complexes with Zn(II) and Al(III) while preserving the more thermodynamically favourable *trans*-configuration of the amidine. To further improve the scope of the FA ligand family, we envisaged a 3rd generation of FA ligands (**C**) for which the amidine function is directly linked to the aryloxy part through the nitrogen atom. Such ligands will form 5- rather than 6-membered metallacycles, which as previously shown by Chen and co-workers in FI series, can enhance the accessibility to the metal and improve catalytic activity.[9,10] Removing the methylene linker between the aryloxy and the amidine fragments will also restore the conjugated character of the ligand. In olefin polymerization catalysis, it has been shown that the π-conjugated character of the FI ligands confers some "electronic flexibility" to the chelated metal active species, and this contributes to the good catalytic performance.[11] Moreover, the conjugated imine and aryloxy moieties generally produce a rigid, nearly planar chelated ring that helps control the coordination sphere around the metal and is certainly of importance in stereocontrolled processes.[2b] One should also note, despite this is beyond the scope of this study, that the conjugated character of FI is a necessary condition for these ligands and their complexes to exhibit interesting photophysical properties for applications in sensors, organic electronics, etc. Herein, we present the synthesis of FA ligands of type **C** and their coordination chemistry toward Zn and Al. Schiff base Al and Zn complexes have been extensively studied as catalysts for the ring-opening polymerization (ROP) of cyclic (di)esters, such as lactide, to give biodegradable polymers.[2c,12] Therefore, we chose this benchmark reaction to test the efficiency of FA complexes.

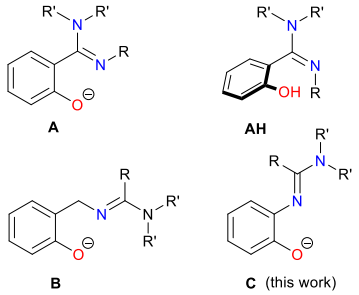

Fig. 1 The different generations of phenoxy-amidine ligands

Results and discussion

Synthesis of the proligands L1H-L6H.

The proligand **L1H** was readily prepared by adapting the procedure previously reported by Hofmann by reacting 2-aminophenol and *N*,*N*-dimethylformamide dimethyl acetal for 10' at 50°C under microwave irradiation (Scheme 1, path a).[13] **L2H** was obtained through the ring opening of benzoxazole by pyrrolidine under solvent-free condition as described by Chang (Scheme 1, path c).[14] We have previously shown that the type-**B** FA ligands incorporating a phenyl group on the amidine-carbon (R = Ph) performs better regarding ROP control.[8] Attempts to synthesize analogous FA type-**C** ligands by reacting 2-aminophenol with the chloroiminium chloride generated from *N*,*N*-dimethylbenzamide and oxalyl chloride led to 2-phenylbenzoxazole. We hypothesized that the phenol-amidine forms in these conditions but undergoes intramolecular cyclisation, as observed with the type-**B** FA ligand, although it was much slower in the latter case.[8] Likewise, reaction targeting a priori more robust FA ligand, with a larger ^{t}Bu group on the amidine-carbon and piperidine NR'$_2$ moiety, also resulted in a cyclization product. On the contrary, reaction of 2-aminophenol with the chloroiminium chlorides prepared from 2-methylbenzamide or 1-naphthylamide derivatives led to the phenol-amidine proligands **L3H-L5H** (Scheme 1, path b). Phenoxy-imines bearing an additional amine functionality have been used by Darensbourg,[15] Shaver,[16] Lin,[17] Mehrkhodavandi,[18] Jones,[19] Mazzeo[20] and others to get highly active Zn-based catalysts in ROP of lactide. An analogous potentially tridentate FA ligand (**L6H**) with a pendant -$(CH_2)_2NMe_2$ arm has been synthesized in one step and with 60% yield using the same strategy as for **L2H**, via the ring opening of benzoxazole by *N*,*N*,*N'*-trimethylethylenediamine.

Suitable crystals for X-ray diffraction studies were obtained for the proligands **L1H**, **L3H**-**L5H**. ORTEP views are represented on Fig. 2. The amidine moieties in the four proligands exhibit a *trans* configuration, sp^2 character for the N2 nitrogen atom ($\Sigma\alpha_{N2} \approx 360°$) and a periplanar conformation ($\theta \approx 0°$) (Table 1). The conjugated character of the amidine group is also reflected by the Δ_{CN} parameters (Δ_{CN} = d(C-N) - d(C=N)) which are in the range 0.043(16) to 0.052(2) Å.[21] The amidine plane is tilted by $126.4(1) \leq |\psi| \leq 169.9(6)°$ with respect to the hydroxyaryl plane, and in the case of **L3H**-**L5H**, is almost orthogonal to the tolyl or naphthyl ring ($80.0(9)° \leq |\alpha| \leq 117.34(15)°$). In addition, intermolecular H-bonds are observed in the solid state structures of **L1H**, **L3H** and **L4H** between the phenolic protons

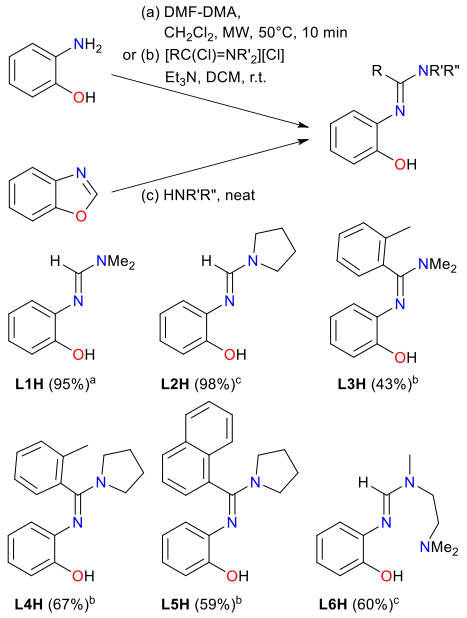

Scheme 1 Synthesis of **L1H**-**L6H** proligands.

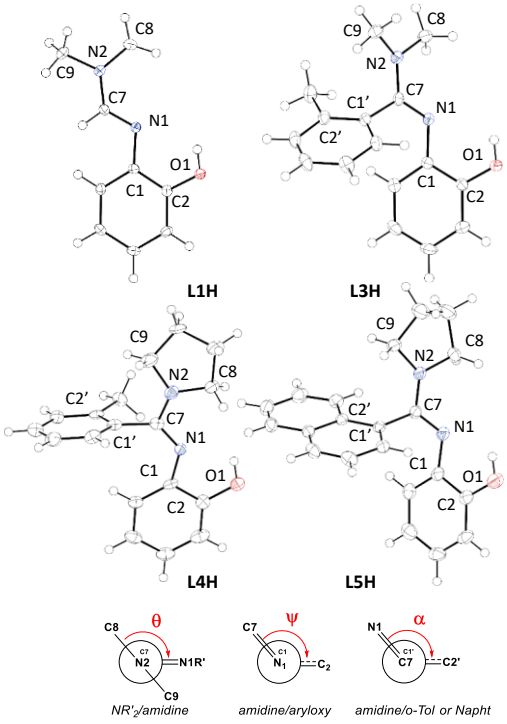

Fig. 2 Views of **L1H, L3H-L5H** (ORTEP, 50% probability ellipsoids; disorder is omitted for clarity)) and definition of torsion angles θ, ψ and α. For relevant bond distances and angles, see Table 1.

Table 1 Relevant bond distances (Å) and angles (°) in the proligands.

	C7-N1	C7-N2	$\Sigma\alpha_{N2}$	θ^a	ψ^b	α^c
L1H	1.290(3)	1.335(3)	359.6(6)	5.0(3)	-143.1(2)	-
L3H	1.304(2)	1.356(2)	357.8(4)	7.0(2)	-128.4(1)	-116.88(15)
L4H	1.305(16)	1.348(8)	359.9(1.7)	0.8(9)	169.9(6)	80.0(9)
L5H	1.298(2)	1.342(2)	360.0(1.8)	1.8(2)	-126.4(1)	117.34(15)

[a]: θ (C8N2C7N1),[b]: ψ (C7N1C1C2), [c]: α (N1C7C1'C2')

and the amidine-*N* atoms of two neighbored molecules oriented in a complementary pairing. The ^{1}H NMR spectra of **L1H**-**L5H** show only one isomer in solution which we assume to be the *trans*-isomer based on solid state structures. The other noticeable point is the number and shape of the NR'R" signal(s) in the ^{1}H NMR spectra of the proligands **L1H**-**L2H** *versus* those of **L3H**-**L5H**. The NMe_2 group in **L1H** gives a broadened singlet at δ = 3.04 ppm ($\Delta\nu_{½}$ = 10.93 Hz) whereas this signal in **L3H** is split into two sharper singlets at δ = 3.25 ppm ($\Delta\nu_{½}$ = 6.86 Hz) and 2.75 ppm ($\Delta\nu_{½}$ = 6.80 Hz). Similarly, the pyrrolidine protons appear as two broad signals in **L2H** whereas they give five well resolved multiplets in **L4H** and **L5H**. This discrepancy can be attributed to the presence of the aryl substituent on the amidine-carbon in **L3H**-**L5H** which impedes the rotation of the C-NR'R" amidine bond and make them non fluxional on the NMR time scale. The ^{1}H NMR spectrum of **L6H** in CD_2Cl_2 shows broad resonances for the methyl protons and two sets of broad signals for both the ethylene and formamidine protons. This observation could be explained by the presence of two rotamers resulting from the presence of two different substituents on the amidine moiety (NR'R") and from the restricted rotation of the amidine bond. Noteworthy, this spectrum becomes simpler in MeOD with only the splitting of the signal due to the methylene attached to the amidine group suggesting a faster interconversion of rotamers in this solvent.[22]

Synthesis of the FA-Al complexes.

The proligands **L1H**-**L6H** were further reacted with one equivalent of $AlMe_3$ in THF at room temperature for 2 hours (Scheme 2). The mono-ligated complexes thus formed were found to undergo redistribution, which prevented their isolation in pure form except in the case of **1a**. Suitable crystals for X-Ray diffraction analysis were obtained for complex **1a** and an ORTEP view is presented on Fig. 3. **1a** exhibits a dimeric structure bridged by the O atoms of the aryloxy ligands and thus differs from previously reported 6-membered ring aluminum FA complexes that crystallize in monomeric form.[8] Other noticeable features are the relatively small O-Al-N angle (79.64(4)°) and long Al-O and Al-N bond distances (d(Al-O) = 1.851(1) Å, d(Al-N) = 2.174(1) Å) in comparison to that found in analogous 6-membered-ring FA aluminum complexes (d(Al-O) = 1.7769(13) Å, d(Al-N) = 1.9601(14) Å, O–Al–N = 96.58(6)°) or in the five 5-membered ring FI aluminum complexes reported by Chen (d(Al-O) = 1.7932(19) Å, d(Al-N) = 2.007(2) Å, O-Al-N = 85.92(8)°).[9a] ^{1}H NMR spectrum of **1a** shows, as characteristic signals, a singlet at δ = 7.76 ppm for the formamidine proton, a single and sharp singlet for the NMe_2 group at δ = 3.25 ppm ($\Delta\nu_{½}$ = 6.80 Hz) and a singlet upfield shifted at δ = 0.73 ppm for the $AlMe_2$ groups. DOSY investigation on a sample of **1a** in CD_2Cl_2 shows a diffusion constant (*D*) equal to 14.5 x 10^{-10} m^2 s^{-1} corresponding to a hydrodynamic radius r_H of 3.65 Å according to the Stokes-Einstein relation. This value is close to that for the monomer estimated from the X-Ray crystallographic data ($r'_{H(monomer)}$ = 3.62 Å, $r'_{H(dimer)}$ = 4.53 Å) indicating that the dimeric form is not retained in solution (See SI, Fig S112). The addition of 2 equivalents of the proligands **L1H**-**L4H** and **L6H** to $AlMe_3$ gave rise to the formation of the bis-ligated complexes **1b**-**4b** and **6b** in 70-91% yields (Scheme 2). The complex obtained from **L5H** could not be isolated in an analytically pure form. Alcoholysis reaction was conducted with **1b** using one equiv. of ^{i}PrOH and afforded the alkoxy Al complex **1b'**. The structure of complexes **1b**-**3b** and **1b'** were determined by X-Ray diffraction analysis (Fig. 4 & 5). Based on geometry indexes the geometries of **1b** and **1b'** can be best described as trigonal bipyramids ($\tau_{5(\mathbf{1b})}$ = 0.69, $\tau_{5(\mathbf{1b'})}$ = 0.76) and those of **2b** and **3b** as intermediates between trigonal bipyramids and square pyramidal geometries ($\tau_{5(\mathbf{2b})}$ = 0.51, $\tau_{5(\mathbf{3b})}$ = 0.40).[23] Continuous shape measure values,[24] confirm the trigonal bipyramidal geometries for **1b** and **1b'** and

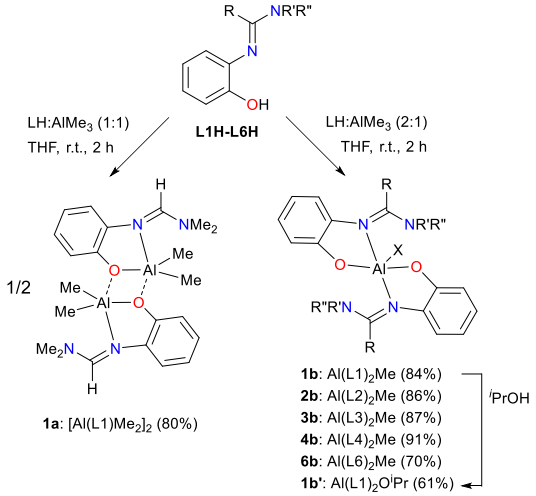

Scheme 2 Synthesis of the FA-Al complexes.

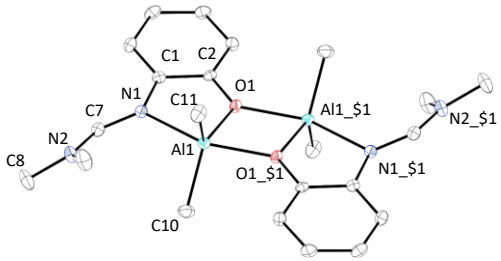

Fig. 3 View of complex **1a** (ORTEP, 50% probability ellipsoids; H atoms are omitted for clarity). For relevant bond distances and angles, see Table 2.

Table 2 Relevant bond distances (Å) and angles (°) in the aluminum complexes.

	C7-N1 C7-N2	Al-Me	Al-O1 Al-N1	τ_5	O1AlN1	θ[a]	ψ[b]
1a	1.309(2) 1.326(2)	1.977(3)	1.851(1) 2.174(1)	0.47	79.64(4)	6.9(2)	-150.99(12)
1b[c]	1.318(4) 1.324(5)	1.980(2)	1.80(1) 2.14(3)	0.69	84.3(2.3)	9.3(2.8)	-156.8(1.2)
1b'[c]	1.312(4) 1.321(1)	-	1.791(6) 2.07(3)	0.76	86.1(3.4)	-7.7(1.0)	151.2(5.0)
2b[c]	1.310(2) 1.322(4)	1.973(2)	1.797(2) 2.121(1)	0.51	82.36(9)	-14.2(1.8)	155.9(1.2)
3b[c]	1.320(1) 1.340(4)	1.970(2)	1.795(2) 2.163(10)	0.40	81.54(17)	-15.45(0.21)	145.42(3)

[a]: θ (C8N2C7N1),[b]: ψ (C7N1C1C2), [c]: the mean values of the two independent molecules are reported.

better match the trigonal bipyramidal geometries for **2b** and **3b** (See Table S95 in SI). The Al-C_{methyl} distances (comprised between 1.970(2) and 1.980(2) Å) and Al-O distances (1.791(6) to 1.80(1) Å) are within the range of analogous FI complexes.[24] The Al-N distances (comprised between 2.07(3) to 2.163(10) Å) are within the longer ones described. The NR'_2 moieties are slightly tilted relative to the amidine plane (6.9(2)°<|θ|<15.45(0.21)°), which itself deviates from the aryloxy plane (145.42(3)°<|ψ|<156.8(1.2)°). In case of **3b**, the bis-ligated complex can exist in the form of three pairs of enantiomers due to both atropisomer axial chirality, generated by the restricted rotation of Csp^2-Csp^2 bond of the aryl moiety, and the chirality at metal (Fig. 5). The ORTEP view of **3b** shows a disorder related to the position, either up or down, of one of the two methyl-tolyl groups, corresponding to the presence of two atropisomers in 3/1 ratio in the crystal (Fig. 5).

^{1}H NMR spectra of complexes **1b**, **2b** and **6b** show diagnostic signals for the formamidine and Al-Me protons in the range 7.97–7.70 and -0.77–-0.79 ppm, respectively. The bis-ligated complexes are chiral-at-metal which is reflected in the ^{1}H NMR spectrum of **1b'** by the presence of two doublets for the diastereotopic isopropyl-methyl groups. VT-NMR experiment was conducted on **1b'** (Fig. 6). When the temperature is raised, the signals of the isopropyl-methyl groups broaden and merge at 348(2.5) K (69.5(5) kJ.mol^{-1}) consistent with the non-persistence of the chiral structure. Within the same range of temperatures, one can also observe the coalescence of the NMe_2 signals (Tc = 343(2.5) K, $\Delta G^{\ddagger}$ = 64.6(5) kJ mol^{-1}) due to rotation about the amidine bond. The ^{1}H NMR spectrum of **3b** in deuterated toluene at room temperature is more complicated and shows 3 sets of signals (Fig. 6), overlapping for some of them, and corresponding to the 3 possible enantiomeric pairs (Fig. 5). A progressive simplification of the

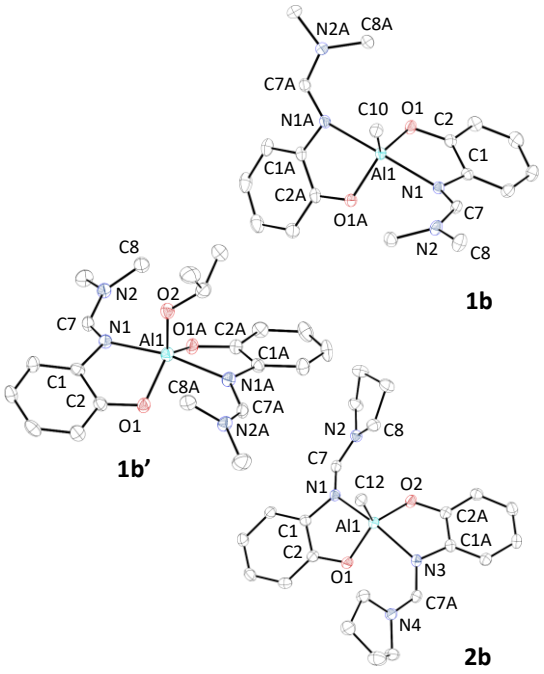

Fig. 4 *Views of complexes **1b, 1b',** and **2b** (ORTEP, 50% probability ellipsoids; H atoms are omitted for clarity). For relevant bond distances and angles, see Table 2.*

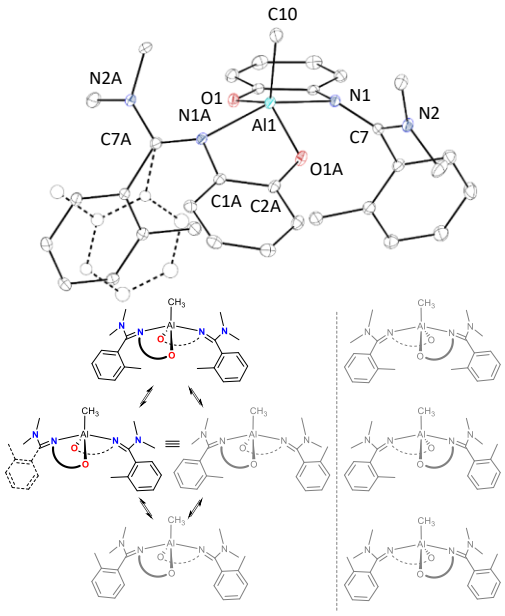

Fig. 5 Top: ORTEP view of complex **3b** where both atropisomers are highlighted (disordered parts: 76%/24%). Thermal ellipsoids are drawn at 25% probability level. Disordered solvents and hydrogen atoms are omitted for clarity). Bottom: Representation of the three possible pairs of enantiomers for complex **3b.** For relevant bond distances and angles, see Table 2.

spectra was observed by raising up the temperature that we interpret as being due initially to the loss of the chirality at Al(Tc* = 308(5) K for the signal at 2.46 ppm, $\Delta G^{\ddagger}$ = 66(1) kJ mol^{-1})and then to a free rotation of the NMe_2 fragment around the amidine bond (Tc** = 346.5(3.5) K, $\Delta G^{\ddagger}$ = 64.6(0.6) kJ mol^{-1}). VT NMR experiment conducted on **3b** in deuterated pyridine from 258 K to 383 K shows first a similar evolution, then the *o*-tolyl-methyl signals broaden and approach coalescence at 383K (Tc***>383 K, $\Delta G^{\ddagger}$>82 kJ mol^{-1}) (See SI, Fig S52). Noteworthy, complex **4b** shows similar NMR behaviour than **3b**. The non-persistence of the chirality at the metal might be explained by decoordination-recoordination process, which was found to occur below 298 K in bis-ligated $AlMe(FI)_2$ complexes.[25]

Synthesis of the FA-Zn complexes.

Zn complexes were obtained *via* an alkane elimination route similar to that in Al series starting from $ZnEt_2$ precursor and the proligand either in 1:1 or 2:1 ratio (Scheme 3). The heteroleptic complexes have a propensity for redistribution in solution which prevented in some cases their isolation in pure form. In fact, only complexes **1c**, **2c**, **5c** and **6c** have been isolated. The hetero- and homoleptic complexes were obtained in 40% to 93% yields and were characterized by NMR (^{1}H, ^{13}C, COSY, HSQC, HMBC), elemental analysis and for some of them X-ray diffraction. In the solid state, the heteroleptic complexes have a dimeric phenoxy-bridged structure and the homoleptic complexes have a spiro structure with the two FA ligands connected to the Zn atom in a C2 symmetric fashion. All the complexes adopt a distorted tetrahedral geometry around the Zn metal ion according to the geometry index $\tau_{4'}$ ranging between 0.70 and 0.79 (Fig 7 and 8).[26] In complexes **6c** and **6d**, the additional ethylene dimethyl

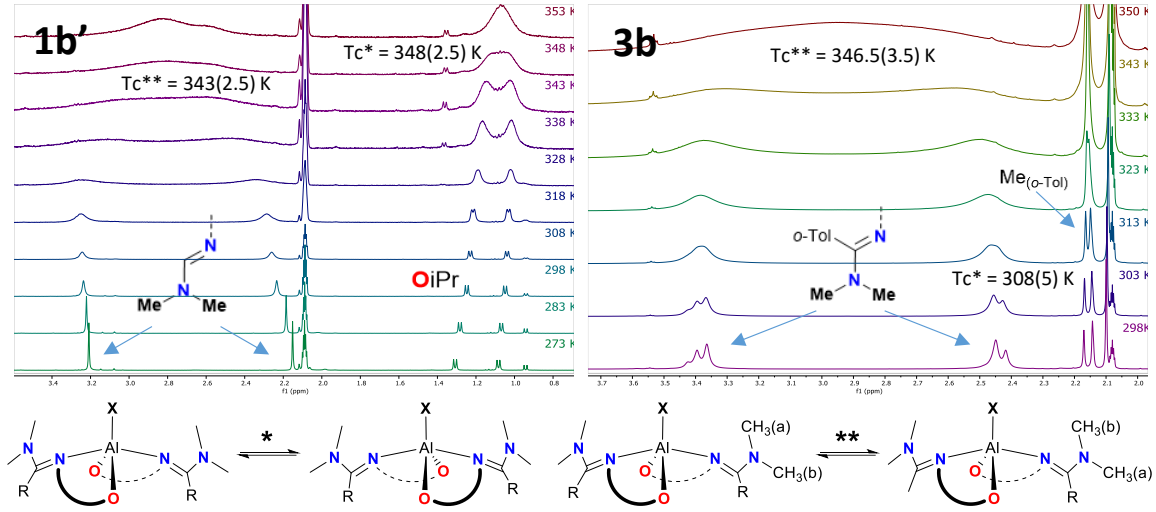

Fig. 6 Top left: stacked ^{1}H NMR spectra (400 MHz, toluene-D_8) of complex **1b'** from 273 K to 353 K. Only the region from 0.7 to 3.6 ppm is shown. Top right: stacked ^{1}H NMR spectra (600 MHz, toluene-D_8) of complex **3b** from 298 K to 350 K. Only the region from 1.6 to 3.6 ppm is shown. Bottom: Dynamic behaviour of **1b'** and **3b** (loss of the chirality at Al (Tc*), rotation of the NMe_2 fragment around the amidine bond (Tc**)).

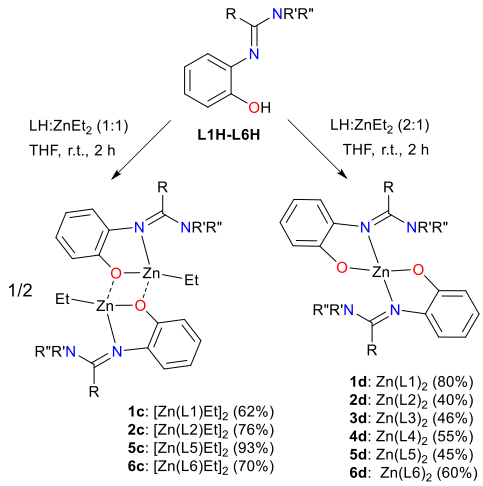

Scheme 3 Synthesis of the FA-Zn complexes.

amine arms are oriented *syn* with respect to the amidine-CH proton and away from the Zn atoms. Inspection of bond distances and angles show values in the range of analogous FI complexes[27] with longer Zn-O1 bond lengths in the O-bridged dimeric complexes than in the monomeric ones and conversely smaller bite angles O1ZnN1 in the former ones. The amidine moieties feature smaller Δ_{CN} values ($0.08(4) \leq \Delta_{CN} \leq 0.037(12)$ Å) in the complexes than in the corresponding proligands. The smallest torsion angles ψ(C7N1C1C2) can be found in complexes **5c**, **3d** and **4d** ($137.4(9)° < |\psi| < 142.0(2)°$) thus showing that the aryl substituent on the amidine carbon greatly contributes to pushing the amidine group out of the aryloxy plane. This is especially true in the case of homoleptic complexes **3d** and **4d**. In line with this, complexes **3d** and **4d** show larger metal-aryloxy plane distances (D = 0.425(2) and 0.43(8) Å) than those in the formamidine FA complexes **1d** and

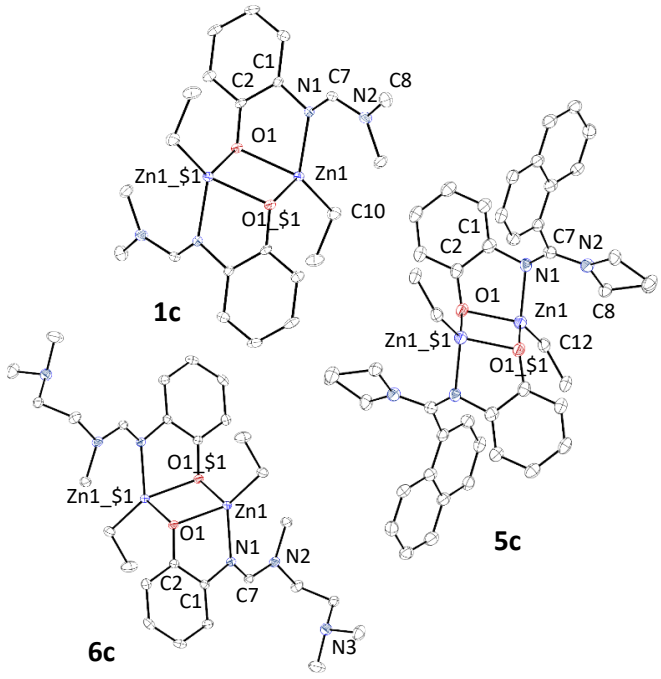

Fig. 7 Views of complexes **1c, 5c, 6c** (ORTEP, 50% probability ellipsoids; H atoms are omitted for clarity). For relevant bond distances and angles, see Table 3.

2d (D = 0.002(2) and 0.131(2) Å). The ^{1}H NMR spectra at 298 K of the heteroleptic complexes show a splitting of the signals for the pyrrolidine ring protons in complex **5c** and only a broadening of the signal(s) for the NR'_2 amidine group in complexes **1c**, **2c** and **6c**. This reveals the impact of the aryl group on the rate of rotation around the amidine bond, as previously observed for the proligands. Moreover, no splitting of the NMe_2 signal is observed in the ^{1}H NMR spectrum of complex **6c** suggesting that the amine arm remains uncoordinated to the Zn metal ion in solution. Noteworthy,

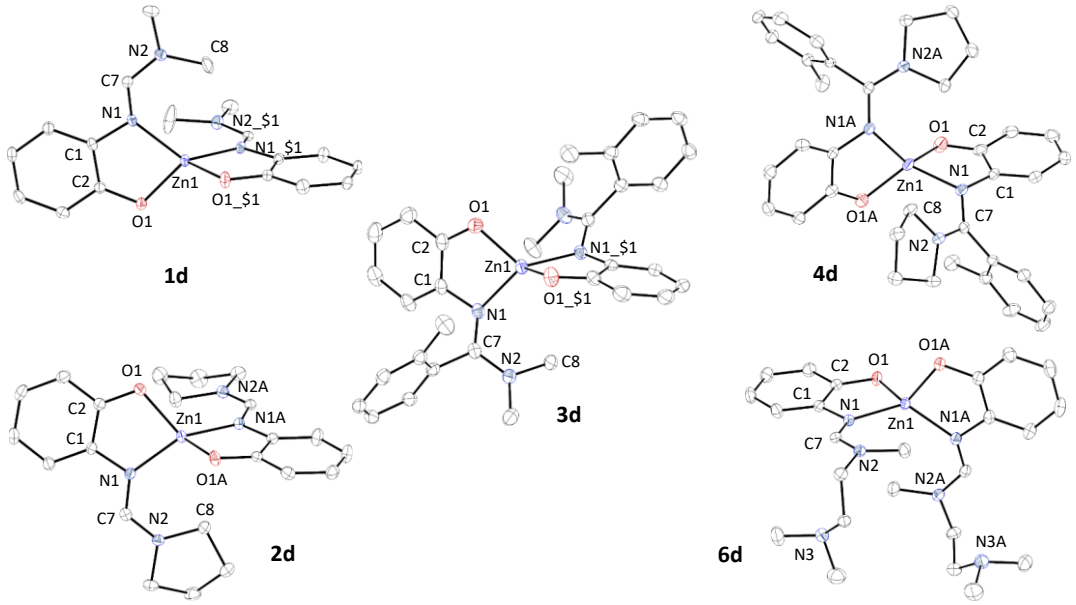

Fig. 8 *Views of complexes **1d-4d** and **6d** (ORTEP, 50% probability ellipsoids; H atoms are omitted for clarity). For relevant bond distances and angles, see Table 3.*

Table 3 Relevant bond distances (Å) and angles (°) in Zn compounds.

	C7-N1	C7-N2	Zn-Et	Zn-O1	Zn-N1	$\tau_{4'}$	D[a]	O1ZnN1	θ[b]	ψ[b]
1c	1.304(4)	1.328(4)	1.970(3)	2.064(2)	2.089(2)	0.71	0.730(3)	80.41(9)	1.3(5)	-151.4(4)
5c[c]	1.307(12)	1.344(12)	1.985(9)	2.047(6)	2.082(7)	0.74	0.80(1)	89.2(11.6)	8.4(14)	-137.4(9)
6c[c]	1.302(2)	1.330(2)	1.978(1)	2.065(6)	2.071(1)	0.70	0.635(1)	91.4(14.9)	3.7(2)	-152.8(1)
1d	1.306(2)	1.323(2)	-	1.934(1)	2.024(1)	0.75	0.002(2)	86.49(5)	0.4(3)	174.5(1)
2d[c]	1.309(3)	1.321(1)	-	1.942(3)	2.009(6)	0.72	0.131(2)	86.76(7)	-2.3(2.1)	177.4(1.2)
3d	1.316(3)	1.339(3)		1.919(1)	2.042(2)	0.77	0.425(2)	86.24(7)	-5.80(3)	142.0(2)
4d[c]	1.325(1)	1.333(4)		1.925(3)	2.047(3)	0.79	0.433(80)	86.30(19)	-5.9(1.8)	146.8(7.8)
6d[c]	1.307(3)	1.329(1)		1.936(2)	2.012(7)	0.75	0.026(11)	86.9(3)	-3.3(6)	171.8(4.6)

[a]: D = mean distance in between Zn atom and the aryloxy plane, [b]: θ (C8N2C7N1) and ψ (C7N1C1C2), [c]: the mean values of the two independent molecules are reported.

DOSY NMR experiment conducted on complex **1c** shows that the dimeric structure is maintained in CD_2Cl_2 but not in deuterated pyridine as shown by the rather good fit between the hydrodynamic radii (r_H), calculated from the diffusion coefficients measured in both solvents, and those estimated (r'_H) from the solid state structure of the complex (CD_2Cl_2, 298 K, D = 11.5 x 10^{-10} $m^2.s^{-1}$, r_H = 4.59 Å, $r'_{H(dimer)}$ = 4.46 Å / Pyridine-D, 298 K, $Đ$ = 6.6 x 10^{-10} $m^2.s^{-1}$, r_H = 3.76 Å, $r'_{H(monomer)}$ = 3.54 Å) (See SI, Fig S113-S114). ^{1}H NMR spectra of complexes **1d** and **2d** show a split of the signals of the NR_2 group due to more hindered motion about the amidine bond in the homoleptic complexes. NMR spectra of complexes **3d**-**5d** in solution at room temperature were rather difficult to interpret due to the presence of several stereoisomers. NMR studies at variable temperatures were carried out for each of these complexes, showing a progressive simplification of the spectra when the temperature was raised up to 383 K (Fig. 9). Given the profile of the spectra, similar to those observed in Al series, we interpret this evolution as being due initially to the loss of chirality at Zn (Tc* = 303(5) K), then to the rotation of the NR'_2 fragment around the amidine bond (Tc** = 323(5) K) and finally to the rotation around the Csp^2-Csp^2 bond of the aryl fragment on the amidine carbon (Tc*** > 383 K). Interestingly, similar values were estimated from Eyring equation for the energy barriers for the epimerization at Zn and Al as for example in complexes **3b** and **3d** (pyridine-D, $\Delta G^{\ddagger}$ = 65(1) kJ mol^{-1}). The ^{1}H NMR spectrum of complex **6d** in CD_2Cl_2 shows sharp singlet at δ = 2.22 ppm ($\Delta\nu_{½}$ = 3.92 Hz) for the NMe_2 protons, and thus no diastereotopic splitting, indicating a bidentate rather than tridentate coordination mode of the FA ligands in solution.

ROP of Lactide.

The Al complexes were evaluated toward the ROP of *rac*-LA in toluene at 90 °C in the presence of isopropanol (Table 4). The dimeric complex **1a** converted 94% of monomer, but the GPC analysis showed a bimodal profile, a large molecular weight distribution and a much smaller Mn than expected. For comparison, a previously reported 6-membered-ring (FA)Al complex, $Al(Me)_2(OC_6H_4(2\text{-}(CH_2\text{–}N{=}C(H)NMe_2)))$, gave similar performances ([LA]:[cat]:BnOH] = 100:1:1, toluene, 70 °C, 24 h, conv. 89% , Mn_{exp} = 3500, $Đ$ = 2.17).[8] The monomeric complexes **1b**-**6b** showed slightly lower activities than **1a**, but yielded PLAs

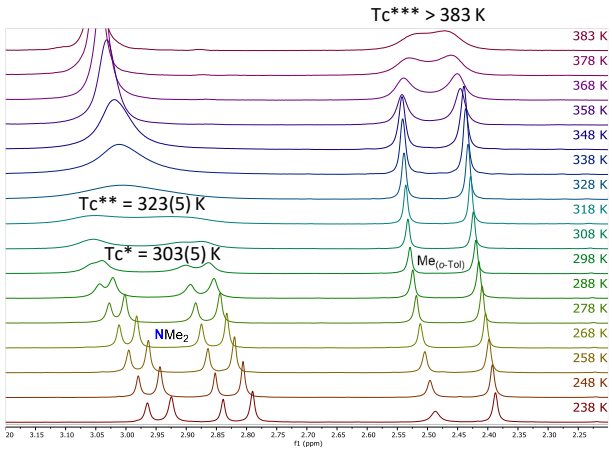

Fig. 9 . Stacked ^{1}H NMR spectra (400 MHz, Pyr-D_5) of complex **3d** from 238 K to 383 K. Only the region from 2.2 to 3.2 ppm is shown. Exchange broadening and coalescence due to loss of the chirality at Zn (Tc*), the rotation of the NMe_2 fragment around the amidine bond (Tc**) and the rotation around the Csp^2-Csp^2 bond of the aryl fragment on the amidine carbon (Tc***).

Table 4 ROP of *rac*-lactide mediated by FA-Al complexes.[a]

Entry	Cat.	Conv. (%)[b]	Mn_{theo}[c]	Mn_{exp}[d]	*Đ*	Pm[e]
1	**1a**	94	13 600	5 400	3.19[f]	0.56
2	**1b**	87	12 300	8 500	1.22	0.61
3	**1b'**[g]	85	12 200	9 600	1.38	0.64
4	**2b**	80	11 400	7 700	1.20	0.56
5	**3b**	87	12 600	8 800	1.30	0.60
6	**4b**	83	11 900	6 100	1.31	0.55
7	**6b**	85	12 300	11 300	1.36	0.57

[a]Polymerization conditions: [*rac*-LA]$_0$ = 1 M, 100 equiv. of *rac*-LA, 1 equiv. of ^{i}PrOH and 1 equiv. of metal catalyst, toluene, 90 °C, 24 h. [b]Monomer conversion. [c]Calculated using $M_{n,theo}$ = [*rac*-LA]$_0$/[catalyst]$_0$ × M_{LA} × conversion. [d]Measured by GPC in THF (45 °C) using PS standards and corrected by applying the appropriate correcting factor (0.58). [e]Determined from the methine region of the HD ^{1}H NMR spectrum. [f]GPC chromatogram presents bimodal profile. [g]Reaction performed in the absence of ^{i}PrOH.

with narrower dispersities and higher number average molecular weights. These Mn values remain, however, smaller than theoretically predicted, except in the case of **6b**. Complex **1b'** gave comparable ROP performance to the two components system **1b**/^{i}PrOH and provided PLA chains terminated with isopropoxy end groups providing evidence that a coordination-insertion mechanism is operating in these conditions (See SI, Fig. S116). Homonuclear decoupled ^{1}H NMR analysis showed slight isotactic bias in PLA produced from *rac*-LA using FA-Al complexes. In comparison with previous reports, the activities of **1b**-**6b** (TOF = 3-4 h^{-1}) are lower than that reported for an analogous pentacoordinated $(FI)_2AlMe$ complex (TOF = 12 h^{-1}) reported by Milione in similar polymerization conditions.[25]

The performances of the Zn complexes for the ROP in solution of *rac*-LA are reported in Table 5. Three FI-Zn complexes **7d**,[28] **8c**,[17a] and **8d**[19] with and without an additional pendant amine arm, were synthesized for comparative purposes (Fig. 10). The polymerization of *rac*-LA (100 equiv.) have been conducted for 2 hours at 20-30 °C in CH_2Cl_2 and in the presence of ^{i}PrOH as co-initiator. Under these conditions, only the hetero- and homoleptic complexes **6c**, **6d** and **8c** derived from FA and FI

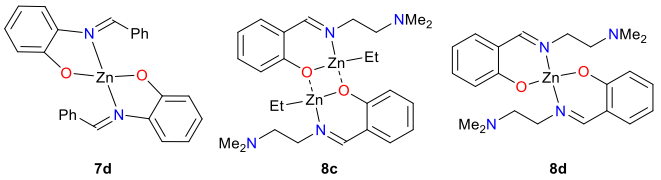

Fig. 10 homo- and heteroleptic FI-Zn complexes **7d**,[28] **8c**[17a] and **8d**[19] synthesized for comparative purposes.

Table 5 ROP of *rac*-lactide mediated by FA-Zn and FI-Zn complexes.[a]

Entry	Cat.	T (°C)	Conv. (%)[b]	Mn_{theo}[c]	Mn_{exp}[d]	*Đ*	Pr[e]
1	**1c**	20	49	7 100	6 400	1.11	0.77
2	**2c**	20	54	7 800	6 800	1.08	0.74
3	**5c**	20	36	5 200	4 500	1.08	0.62
4	**6c**	20	90	13 000	10 900	1.13	0.57
5	**8c**	20	93	13 400	11 500	1.04	0.65
6	**1d-5d**	30	0	-	-	-	-
7	**6d**	30	86	12 400	11 200	1.11	0.62
8	**7d**	30	0	-	-	-	-
9	**8d**	30	52	7 500	5 800	1.05	n.d.

[a]Polymerization conditions: [*rac*-LA]$_0$ = 1 M, 100 equiv. of *rac*-LA, 1 equiv. of ^{i}PrOH and 1 equiv. of metal catalyst, CH_2Cl_2, 2 h. [b]Monomer conversion. [c]Calculated using $M_{n,theo}$ = [*rac*-LA]$_0$/[catalyst]$_0$ × M_{LA} × conversion. [d]Measured by GPC in THF (45 °C) using PS standards and corrected by applying the appropriate correcting factor (0.58). [e]Determined from the methine region of the HD ^{1}H NMR spectrum (See SI, Fig. S115).

ligands with a pendant amine arm, led to high monomer conversions. SEC analysis of the resulting PLA showed chains with narrow dispersities and Mn values that match well with those predicted theoretically on the basis of monomer-catalyst ratio and conversion. Other heteroleptic complexes **1c**, **2c** and **5c** produced also chain-length controlled and narrowly disperse PLA but with lower conversions (36-54%). These results differ from those obtained previously with 6-membered ring Zn (FA) complexes ($[(OC_6H_4(2\text{-}(CH_2\text{-}N{=}C(R)NR'_2))Zn(Et)]_2$), which gave higher monomer conversions but broader dispersities, except for the FA ligand, which incorporates a phenyl group and a pyrrolidine on the amidine moiety. Heteroleptic FA Zn complexes thus appear to follow a trend opposite to that of FI complexes, for which five-membered ring systems show higher activity in ROP of ε-caprolactone than the six-membered ring Zn complexes.[27] The homoleptic complexes **1d**-**5d** showed no activity for the ROP of *rac*-LA at 30 °C in the presence of ^{i}PrOH. Complex **7d** showed no activity at 30 °C in CH_2Cl_2 while **8d** provided PLA with 52 % conversion after 2 h. Consistent with previous works in the literature,[20] these results highlight the crucial role of the additional amine arm for FI ligands and this generation of FA ligands in homoleptic Zn complexes to obtain an active ROP catalyst in solution. With regard to tacticity, it should be noted that FA-Zn complexes differ from their Al counterparts in producing PLA with a heterotactic rather than isotactic bias. Kinetic data for complexes **6c** and **6d** are gathered on Fig. 11 and show pseudo first order consumption of LA *vs* time with a higher rate constant for the heteroleptic complex (k_{app} = 0.030 ± 0.007 min^{-1}) than for the homoleptic ones (k_{app} =

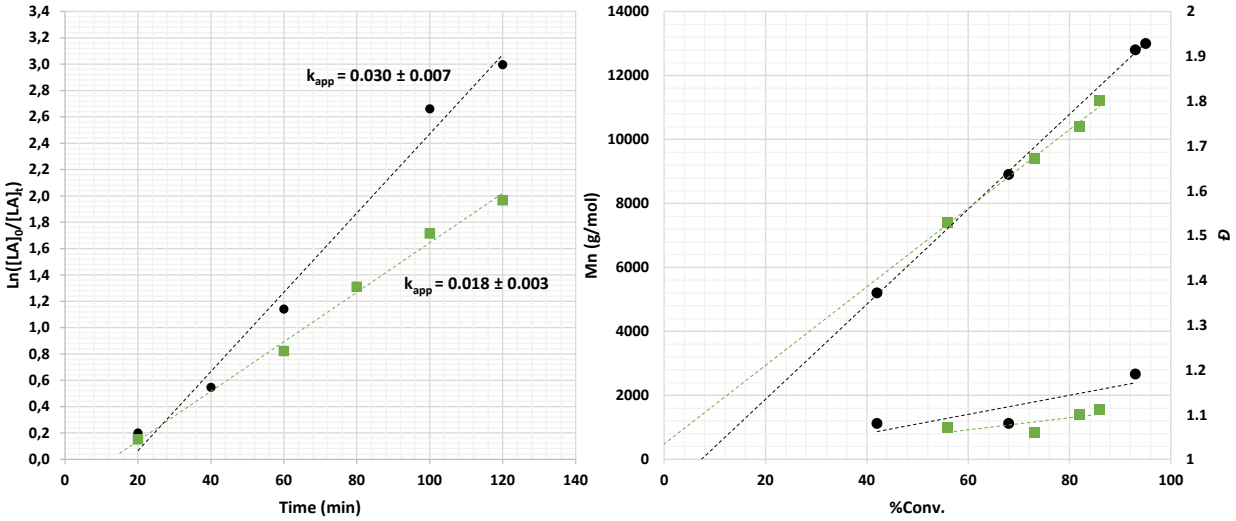

Fig. 11 . *Left: First-order logarithmic plot for the polymerization of rac-LA at 25°C in CH_2Cl_2 using **6c** (●) and **6d** (■) with ^{i}PrOH as initiators (100:1:1). Right: M_n and PDI against conversion associated with the kinetic studies of **6c** (●) and **6d** (■) with ^{i}PrOH.*

Table 6 ROP of *rac*-lactide mediated in bulk conditions by FA-Zn and FI-Zn complexes.[a].

Entry	Cat.	Ratio	T (°C)	T (min)	Conv. (%)[b]	Mn_{theo}[c]	Mn_{exp}[d]	*Đ*	Pr[e]
1	**1c**	[300:1:1]	130	10	82	35 000	28 200	2.82	0.61
2	**2c**	[300:1:1]	130	10	96	41 500	24 800	2.38	0.57
3	**5c**	[300:1:1]	130	10	94	40 600	17 900	1.85	0.56
4	**6c**	[300:1:1]	130	10	95	41 100	30 900	3.15	0.55
5	**6c**	[300:1:1]	130	2	73	31 600	39 800	2.72	0.53
6	**8c**	[300:1:1]	130	2	74	32 000	25 100	3.02	0.59
7	**1d**	[300:1:1]	130	30	73	31 600	16 100	1.17	0.71
8	**2d**	[300:1:1]	130	30	43	18 600	9 500	1.08	0.70
9	**3d**	[300:1:1]	130	2	44	19 000	12 800	1.09	0.58
10	**4d**	[300:1:1]	130	2	42	18 200	10 900	1.17	0.57
11	**5d**	[300:1:1]	130	2	58	24 900	9 900	1.15	0.62
12	**6d**	[300:1:1]	130	2	65	28 100	14 800	1.21	0.53
13	**6d**	[1000:1:10]	130	5	95	13 700	9 600	1.18	0.57
14	**6d**	[1000:1:10]	180	2	93	13 400	13 200	1.47	n.d.
15	**7d**	[300:1:1]	130	2	48	20 800	14 800	1.12	0.61
16	**8d**	[300:1:1]	130	2	42	18 200	8 700	1.07	0.59

[a]Polymerization conditions: free-solvent conditions, Ratio = [number of equiv. of *rac*-LA: number of equiv. of metal catalyst : number of equiv.of BnOH]. [b]Monomer conversion. [c]Calculated using $M_{n,theo}$ = [*rac*-LA]$_0$/[catalyst]$_0$ × M_{LA} × conversion. [d]Measured by GPC in THF (45 ˚C) using PS standards and corrected by applying the appropriate correcting factor (0.58). [e]Determined from the methine region of the HD ^{1}H NMR spectrum.

0.018 ± 0.003 min^{-1}). A linear relationship between Mn values and the percentage of conversion of LA was also observed for both complexes and agree with well-controlled ROP processes. MALDI-TOF analysis of short PLA chains obtained after a short reaction time (40') using **6c** and **6d** in the presence of ^{i}PrOH as a co-initiator showed isopropoxy-terminated chains with a peak spacing of 144 Da and no intercalated peak due to secondary transesterification reactions. Nevertheless, a propensity for transesterification was observed for both complexes at higher monomer conversions (See SI, Fig. S117-S120).

The zinc complexes were then tested under solvent-free conditions, which has the advantage of being closer to industrial PLA production conditions (Table 6). The four heteroleptic FA Zn complexes **1c**, **2c**, **5c** and **6c,** in combination with BnOH, yielded PLA after 10 min at 130°C with high conversions, moderate molecular weight control and broad molecular weight distributions (*Đ* = 1.85-3.15). Further reaction carried out with complex **6c** and stopped after only 2 min led to a lower conversion but similar dispersity, ruling out the hypothesis that the lack of polymerization control was due to side transesterification reactions occurring at the end of the ROP process. Noteworthy, the heteroleptic FI Zn complex **8c** showed similar performance in these conditions. The homoleptic complexes **1d**-**6d** were all active for the ROP of *rac*-LA in bulk conditions at 130 °C. Complexes **1d** and **2d** with formamidine-based FA ligands were less active than complexes **3d**-**5d** featuring an aryl substituent on the amidine carbon. Complex **6d**, with two pendant amine arms, led to the highest activity.

SEC analysis showed much narrower molecular weight distributions for the PLA chains obtained with the homoleptic Zn complexes than with the heteroleptic ones, but Mn values lower than predicted. Tests carried out in parallel with the homoleptic FI Zn complexes **7d** and **8d**, previously reported by Jones, show that the FA and FI Zn homoleptic complexes give similar performance. The most active initiator **6d** was next tested in transfer chain conditions at lower catalyst loading ([LA]:[**6d**]:[BnOH] = 1000:1:10). Under these conditions, **6d** afforded narrow disperse PLA chains with predictable Mn values and almost complete conversions of LA after 5 min at 130°C and after 2 min at 180°C.

Conclusions

In conclusion, the synthesis of FA ligands featuring a trisubstituted amidine *N*-linked to an aryloxy moiety is described. This new generation of FA ligands was found suitable to form chelate complexes with Al and Zn metal ions. Alkane metathesis route from the phenol-amidine proligand and aluminum or zinc alkyls was used and led to mono-ligated and bis-ligated complexes. The latter exhibit fluxional behaviour in solution, attributed to the hemilability of the FA ligand and the rotation around the C-NR'_2 and C-Ar bonds of the amidine moiety. ROP catalytic tests of *rac*-LA in solution show that both Al and Zn complexes featuring FA ligands with a pendant amine arm perform best, following a similar trend to the parent FI complexes. On the other hand, the use of this new generation of FA ligands that form a 5-membered metallacycle rather than a 6-membered metallacycle did not contribute to improved ROP catalytic activities, contrary to what was previously observed in the FI series. However, these third-generation FA complexes are still quite competitive with their FI counterparts. Lastly, the homoleptic Zn complexes were successfully employed for ROP of *rac*-LA under free-solvent condition at 130-180°C and using BnOH as co-initiator. The best complex was again found to be complex **6d** incorporating a pendant amine arm on the FA ligands, although the gap with other complexes was less significant in these harsher conditions.

Experimental

General consideration.

All reactions, except when indicated, were carried out under an atmosphere of argon using conventional Schlenk techniques and Ar glovebox. DCM, diethyl ether, THF, toluene, and pentane were dried using a MBRAUN SPS 800. Analyses were performed at the "Plateforme d'Analyses Chimiques de Synthèse Moléculaire de l'Université de Bourgogne". Elemental analyses were performed by Mr Marcel Soustelle and Ms Tiffanie Régnier on CHNS ThermoFisher Scientific Flash EA 1112 analyzer. A satisfactory elemental analysis could not be obtained for the complexes **1b**, **2b**, **4b**, **1c** and **5c**, possibly due to partial hydrolysis out of the glovebox. Reagents were commercially available and used as received. High resolution mass spectra were recorded on a Thermo LTQ Orbitrap XL ESI-MS

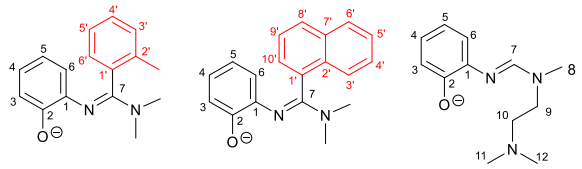

Fig. 12 Numbering of C / H atoms in FA ligands.

(ElectroSpray Ionization Mass Spectrometry). All X-Ray experimental procedure and crystal data are detailed in SI. NMR spectra (^{1}H, ^{13}C) were recorded on Bruker 400 Avance Neo, Bruker 500 Avance Neo, or Bruker 600 Avance HD spectrometers. Chemical shifts are quoted in parts per million (δ) relative to TMS (for ^{1}H and ^{13}C). For ^{1}H and ^{13}C spectra, values were determined by using solvent residual signals (*e.g.* $CHCl_3$ in $CDCl_3$) as internal standards. The apparent multiplicity of the ^{1}H signals is reported. Assignment of ^{1}H and ^{13}C signals (when possible) was done through the use of 2D experiences (COSY, HSQC and HMBC). Nomenclature: the positions of carbon and hydrogen atoms in FA ligands were labelled according to Fig. 12. The proligand **L2H** was synthesized according to previously reported procedure.[14] The synthesis of **7d**[28] is described in SI (S59).

Synthesis of *N'*-(2-hydroxyphenyl)-*N*,*N*-dimethylformamidine L1H.

5 mL dichloromethane solution containing 250 mg (2.3 mmol) of 2-aminophenol and 274 mg (2.3 mmol, 1 equiv.) of DMF-DMA was heated in a microwave synthesis reactor for 10 minutes at 50 °C. The solvent was removed under vacuum to give **L1H** as an orange powder (358 mg, 95% yield). ^{1}H NMR (400 MHz, CD_2Cl_2, 298 K): δ (ppm) = 7.77 (s, 1H, H7), 6.91 (dd, *J* = 7.7, 1.5 Hz, 1H, H6), 6.90-6.84 (m, 1H, H4), 6.82 (dd, *J* = 7.9, 1.6 Hz, 1H, H3), 6.75 (td, *J* = 7.5, 1.7 Hz, 1H, H5), 3.04 (broad s ($\Delta\nu_{½}$ = 10.9 Hz), 6H, $N\underline{Me}_2$). {^{1}H}^{13}C NMR (101 MHz, CD_2Cl_2, 298 K): δ (ppm) = 153.07 (C7), 150.63 (C2), 137.88 (C1), 123.65 (C4), 120.08 (C5), 115.71 (C6), 113.38 (C3), 40.66 ($N\underline{Me}_2$), 34.72 ($N\underline{Me}_2$). Elemental Analysis: calcd for $C_9H_{12}N_2O$: C, 65.83; H, 7.37; N, 17.06. Found: C, 65,43; H, 7.14; N, 16.63. HR-MS (ESI-pos): calcd for $[C_9H_{13}N_2O]^+$ [M + H]$^+$: 165.10224. Found: 165.10167. Δ = -3.452 ppm.

Synthesis of *N'*-(2-hydroxyphenyl)-*N*,*N*-pyrrolidinyl-formamidine L2H.

150 mg of benzoxazole (1.26 mmol, 1 equiv.) was totally dissolved in 210 µL of pyrrolidine (2 equiv.). We stirred at room temperature during 15 minutes. Then, the homogenous solution was dried under vacuum and to afford a white powder (235 mg, yield 98%). ^{1}H NMR (400 MHz, CD_2Cl_2, 298 K): δ(ppm) = 8.02 (s, 1H, H7), 6.92 (m, 1H, H6), 6.86 (m, 1H, H4), 6.81 (m, 1H, H3), 6.74 (m, 1H, H5), 3.53 (s, 4H, Pyrr.), 1.96 (s, 4H, Pyrr.). Data in agreement with literature. {^{1}H}^{13}C NMR (101 MHz, CD_2Cl_2, 298 K): δ(ppm) = 150.70 (C2), 149.80 (C7), 138.15 (C1), 123.46 (C4), 120.01 (C6), 115.40 (C5), 113.29 (C3), 49.33 (Pyrr.), 45.80 (Pyrr.), 25.63 (Pyrr.), 25.08 (Pyrr.). Elemental Analysis: calcd for $C_{11}H_{14}N_2O$: C, 69.45; H, 7.42; N, 14.73. Found: C, 69.67; H, 7.56;

N, 14.51. HR-MS (ESI-pos): calcd for $[C_{11}H_{15}N_2O]^+$ [M + H]$^+$: calcd 191.11798. Found 191.11710. Δ = -4.134 ppm.

Synthesis of *N'*-(2-hydroxyphenyl)-*N*,*N*-dimethyl-2-methylbenzamidine L3H.

Under argon, 1.4 g (8.6 mmol) of 2-methylbenzamide was dissolved into 40 mL of dried toluene. 3.7 mL (43 mmol, 5 equiv.) of oxalyl chloride was then slowly added at 0°C. The solution was then allowed to reach r.t. and heated at 60°C overnight. Volatiles were evaporated and the crude whitish powder was washed with 3x30 mL of dried Et_2O. The resulting chloroiminium chloride was solubilized again in 90 mL of dried CH_2Cl_2. 6 mL (43 mmol, 5 equiv.) of triethylamine were added and the mixture was cooled to 0°C. 938 mg (8.6 mmol, 1 equiv.) of 2-aminophenol were added and the solution was allowed to reach r.t. and stirred for 1 h. The volatiles were evaporated and the residue was taken back into 90 mL of diethyl ether. A 1M solution of HCl in diethyl ether was added until pH = 1 and the amidinium salt was then filtrated under vacuum. The solid was suspended into 30 mL of CH_2Cl_2 and aqueous NH_3 was added until pH = 9-10. The solution was dried over $MgSO_4$ and evaporated under vacuum. The crude product was purified by column chromatography on alumina using CH_2Cl_2 first, and then a 50/1 CH_2Cl_2/MeOH mixture, affording **L3H** as a pale orange solid (940 mg, 43% yield). ^{1}H NMR (600 MHz, CD_2Cl_2, 298 K): δ(ppm) = 7.26 (td, *J* = 7.4, 1.4 Hz, 1H, H4'), 7.19 (overlapping signals, 2H, H3' and H5'), 7.08 (dd, *J* = 8.0, 1.4 Hz, 1H, H6'), 6.74 (dd, *J* = 7.9, 1.5 Hz, 1H, H3), 6.67 (td, *J* = 7.7, 1.5 Hz, 1H, H4), 6.32 (td, *J* = 7.6, 1.5 Hz, 1H, H5), 5.98 (dd, *J* = 7.9, 1.5 Hz, 1H, H6), 3.25 (broad s ($\Delta\nu_{½}$ = 6.9 Hz), 3H, N$\underline{Me}_2$), 2.75 (broad s ($\Delta\nu_{½}$ = 6.8 Hz), 3H, N$\underline{Me}_2$), 2.12 (s, 3H, *o*-C$\underline{H}_3$). {^{1}H}^{13}C NMR (150 MHz, CD_2Cl_2, 298 K): δ(ppm) = 161.94 (C7), 150.60 (C2), 136.77 (C1), 135.92 (C2'), 134.15 (C1'), 130.63 (C3'), 129.32 (C4'), 128.57 (C6'), 126.31 (C5'), 122.76 (C4), 120.32 (C6), 119.12 (C5), 112.81 (C3), 38.86 (N$\underline{Me}_2$), 37.36 (N$\underline{Me}_2$), 19.24 (*o*-C$\underline{H}_3$). Elemental Analysis: calcd for $C_{16}H_{18}N_2O$: C, 75.56; H, 7.13; N, 11.01. Found: C, 75.32; H, 7.75; N, 11.11. HR-MS (ESI-pos): calcd for $[C_{16}H_{19}N_2O]^+$ [M + H]$^+$: 255.14919. Found: 255.14830. Δ = -3.488 ppm.

Synthesis of *N'*-(2-hydroxyphenyl)-*N*,*N*-pyrrolidinyl-2-methylbenzamidine L4H.

1.65 g (8.7 mmol) of *N*,*N*-pyrrolidinyl-2-methylbenzamide were charged in a Schlenk tube and solubilized in 40 mL of dried toluene. 3.2 mL (37.4 mmol, 4.3 equiv.) of oxalyl chloride were added at 0°C. The solution was allowed to reach r.t. and then heated at 60°C overnight. After cooling the reaction mixture to r.t., 40 mL of dried diethyl ether were added and solvents were removed by filtrating cannula. The white solid was further washed twice with 40 mL of dried diethyl ether and then dried under vacuum for 5 h. The chloroiminium chloride intermediate was taken back in 80 mL of dried dichloromethane. 6.1 mL (43.5 mmol, 5 equiv.) of triethylamine and 949 mg (8.7 mmol, 1 equiv.) of 2-aminophenol were successively added at 0°C. The mixture was allowed to reach r.t. and stirred for 1.5 h before being hydrolyzed by 80 mL of distilled water. The product was extracted with dichloromethane and the organic phase was dried over $MgSO_4$, before being evaporated under vacuum. The crude product was purified by column chromatography on alumina, using a 50/1 CH_2Cl_2/MeOH mixture as the eluent, affording **L4H** (1.6 g, 67% yield). ^{1}H NMR (600 MHz, CD_2Cl_2, 298 K): δ(ppm) = 7.27 (td, *J* = 7.5, 1.5 Hz, 1H, H4'), 7.23-7.17 (overlapping signals, 2H, H3' + H5'), 7.15 (dd, *J* = 7.5, 1.5 Hz, 1H, H6'), 6.74 (dd, *J* = 7.9, 1.5 Hz, 1H, H3), 6.66 (td, *J* = 7.6, 1.5 Hz, 1H, H4), 6.31 (td, *J* = 7.7, 1.5 Hz, 1H, H5), 6.03 (dd, *J* = 7.9, 1.5 Hz, 1H, H6), 3.73 (t, *J* = 7.0 Hz, 2H, Pyrr.), 3.14-3.08 (m, 1H, Pyrr.), 2.99-2.94 (m, 1H, Pyrr.), 2.12 (s, 3H, *o*-C$\underline{H}_3$), 2.05-1.98 (m, 2H, Pyrr.), 1.92-1.80 (m, 2H, Pyrr.). {^{1}H}^{13}C NMR (150 MHz, CD_2Cl_2, 298 K): δ(ppm) = 159.48 (C7), 150.70 (C2), 136.68 (C1), 135.52 (C1'), 135.22 (C2'), 130.70 (C3'), 129.24 (C4'), 128.09 (C6'), 126.38 (C5'), 122.61 (C4), 120.16 (C6), 119.03 (C5), 112.72 (C3), 48.69 (Pyrr.), 47.36 (Pyrr.), 26.24 (Pyrr.), 25.18 (Pyrr.), 19.21 (*o*-C$\underline{H}_3$). Elemental Analysis: calcd for $(C_{18}H_{20}N_2O)_{100}(CH_2Cl_2)_2$: C, 76.73; H, 7.16; N, 9.93. Found: C, 76.35; H, 7.12; N, 10.10. HR-MS (ESI-pos): calcd for $[C_{18}H_{21}N_2O]^+$ [M + H]$^+$: 281.16484. Found: 281.16397. Δ = -3.094 ppm.

Synthesis of *N'*-(2-hydroxyphenyl)-*N*,*N*-pyrrolidinyl-1-naphthylamidine L5H.

This compound was prepared similarly to **L4H** starting with *N*,*N*-pyrrolidinyl-1-naphthylamide (2.2 g, 11 mmol). **L5H** was isolated as an orange solid (1.9 g, 59% yield). ^{1}H NMR (600 MHz, CD_2Cl_2, 298 K): δ(ppm) = 7.92-7.85 (overlapping signals, 2H, H5' + H8'), 7.84-7.79 (m, 1H, H3'), 7.56-7.49 (overlapping signals, 2H, H4' + H6'), 7.45 (dd, *J* = 8.3, 7.0 Hz, 1H, H9'), 7.30 (dd, *J* = 7.0, 1.2 Hz, 1H, H10'), 6.70 (dd, *J* = 7.9, 1.5Hz, 1H, H3), 6.56 (td, *J* = 7.7, 1.5 Hz, 1H, H4), 6.10 (td, *J* = 7.7, 1.5 Hz, 1H, H5), 5.88 (dd, J = 7.9, 1.5 Hz, 1H, H6), 3.93-3.82 (m, 2H, Pyrr.), 3.08-3.00 (m, 1H, Pyrr.), 2.92-2.86 (m, 1H, Pyrr.), 2.08-2.01 (m, 2H, Pyrr.), 1.88-1.75 (m, 2H, Pyrr.). {^{1}H}^{13}C NMR (150 MHz, CD_2Cl_2, 298 K): δ(ppm) = 158.74 (C7), 150.53 (C2), 136.93 (C1), 133.77 (C1'/C7'), 133.65 (C1'/C7'), 130.55 (C2'), 129.47 (C5'/C8'), 128.99 (C5'/C8'), 127.63 (C4'/C6'), 126.77 (C10'), 126.08 (C4' /C6'), 125.72 (C9'), 125.08 (C3'), 122.64 (C4), 120.00 (C6), 118.95 (C5), 112.74 (C3), 48.52 (Pyrr.), 47.67 (Pyrr.), 26.21 (Pyrr.), 25.18 (Pyrr.). Elemental Analysis: calcd for $(C_{21}H_{20}N_2O)_{100}(CH_2Cl_2)_5$: C, 78.85; H, 6.32; N, 8.74. Found: C, 78.41; H, 6.40; N, 8.90. HR-MS (ESI-pos): calcd for $[C_{21}H_{21}N_2O]^+$ [M + H]$^+$: 317.16484. Found: 317.16510. Δ = -0.820 ppm.

Synthesis of L6H.

299.3 mg of benzoxazole (2.4 mmol) were placed in an Eppendorf, and 0.62 mL (490.5 mg, 4.8 mmol, 2 equiv.) of N,N,N'-trimethylethylenediamine was added. The mixture was stirred at 60 °C for 2 h. The crude product was then purified by column chromatography on alumina column with a 10/1 DCM/MeOH mixture to afford 316 mg of **L6H** (60% yield). ^{1}H NMR (400 MHz, MeOD, 298 K): δ(ppm) = 7.76 (s, 1H, H7), 6.93-6.80 (overlapping signals, 2 H, H4 + H6), 6.80-6.68 (overlapping signals, 2H, H3 + H5), 3.61 (overlapping signals, 2H, H9), 3.04 (broad signal, 3H, H8), 2.56 (broad signals, 2H, H10), 2.30 (broad signals, 6 H, H11 + H12). {^{1}H}^{13}C NMR (100.6 MHz, MeOD, 298 K): δ(ppm) = 155.78 (C7), 151.42 (C2), 139.34 (C1), 124.54 (C4/C6), 120.82 (C3/C5), 120.00 (C4/C6), 115.18 (C3/C5), 58.35 (C10), 52.12 (C9), 45.67 (C11 + C12), 33.08 (C8). Elemental

Analysis: calcd for $C_{12}H_{19}N_3O$: C, 65.13; H, 8.65; N, 18.99 . Found: C, 64.53; H, 8.63; N, 18.89. HR-MS (ESI-pos): calcd for $[C_{12}H_{20}N_3O]^+$ $[M + H]^+$: 222.16009. Found: 222.15987. Δ = -0.990 ppm.

Synthesis of 1a.

In a glovebox, 98 mg (0.6 mmol) of **L1H** were solubilized in 6 mL of dried THF. 0.3 mL (0.6 mmol, 1 equiv.) of a 2 M solution of $AlMe_3$ in hexane was added and the mixture was stirred at r.t. for 2h. The volatiles were evaporated under vacuum and the solid product was then washed with 3 mL of pentane. The whitish residue was dried under vacuum affording **1a** as a whitish powder (105 mg, 80% yield). ^{1}H NMR (400 MHz, CD_2Cl_2, 298 K): δ(ppm) = 7.76 (s, 1H, H7), 6.97 (td, *J* = 7.7, 1.5 Hz, 1H, H4), 6.90-6.83 (overlapping signals, 2H, H3 + H6), 6.68 (td, *J* = 7.6, 1.5 Hz, 1H, H5), 3.25 (broad s ($\Delta\nu_{½}$ = 11.0 Hz), 6H, N$\underline{Me}_2$), -0.73 (6H, s, Al$\underline{Me}_2$). {^{1}H}^{13}C NMR (101 MHz, CD_2Cl_2, 298 K): δ(ppm) = 156.39 (C7), 154.01 (extracted form HMBC, C2), 137.73 (extracted from HMBC, C1), 125.96 (C4), 118.00 (C5), 116.67 (C3), 115.46 (C6), 43.30 (N$\underline{Me}_2$, extracted from HSQC), 38.54 (N$\underline{Me}_2$, extracted from HSQC), -6.82 (Al$\underline{Me}_2$). Elemental Analysis: calcd for $C_{11}H_{17}AlN_2O$: C, 59.99; H, 7.78; N, 12.72. Found: C, 59.53; H, 8.97; N, 13.03.

Synthesis of 1b.

In a glovebox, 131 mg (0.8 mmol) of **L1H** were solubilized in 6 mL of dried THF. 0.2 mL (0.4 mmol, 0.5 equiv.) of a 2 M solution of $AlMe_3$ in hexane was added and the mixture was stirred at r.t. for 2h. The volatiles were evaporated under vacuum and the solid product was then washed with 3 mL of pentane. The whitish residue was dried under vacuum affording 117 mg of pure complex as a whitish powder (84% yield). ^{1}H NMR (400 MHz, CD_2Cl_2, 298 K): δ(ppm) = 7.70 (s, 2H, H7), 6.89 (td, *J* = 7.6, 1.6 Hz, 2H, H4), 6.81 (dd, *J* = 7.8, 1.6 Hz, 2H, H6), 6.68 (dd, *J* = 7.9, 1.4 Hz, 2H, H3), 6.59 (td, *J* = 7.6, 1.5 Hz, 2H, H5), 3.41 (broad s ($\Delta\nu_{½}$ = 36.7 Hz), 6H, N$\underline{Me}_2$), 3.21 (broad s ($\Delta\nu_{½}$ = 36.2 Hz), 6H, N$\underline{Me}_2$), -0.79 (3H, s, Al$\underline{Me}$). {^{1}H}^{13}C NMR (101 MHz, CD_2Cl_2, 298 K): δ(ppm) = 156.10 (C7 + C2 overlapping), 139.44 (C1), 125.22 (C4), 116.96 (C5), 115.91 (C3), 115.32 (C6), 43.09 (N$\underline{Me}_2$), 38.51 (N$\underline{Me}_2$), -4.74 (deducted from HSQC, Al$\underline{Me}$). Elemental Analysis: calcd for $C_{19}H_{25}AlN_4O_2$: C, 61.94; H, 6.84; N, 15.21. Found: C, 61.20; H, 7.64; N, 15.41.

Synthesis of 2b.

This compound was prepared similarly to **1b** using **L2H** ligand (190 mg, 1 mmol). Complex **2b** was isolated as a whitish powder (180 mg, 86% yield). ^{1}H NMR (400 MHz, CD_2Cl_2, 298 K): δ(ppm) = 7.97 (s, 2H, H7), 6.92-6.80 (overlapping signals, 4H, H4 and H6), 6.68 (dd, *J* = 7.8, 1.5 Hz, 2H, H3), 6.59 (td, *J* = 7.6, 1.5 Hz, 2H, H5), 4.39 (broad ($\Delta\nu_{½}$ = 32.7 Hz), 2H, Pyrr.), 3.93-3.54 (broad, 6H, Pyrr.), 1.99 (broad ($\Delta\nu_{½}$ = 17.7 Hz), 8H, Pyrr.), -0.77 (s, 3H, AlMe). {^{1}H}^{13}C NMR (101 MHz, CD_2Cl_2, 298 K): δ(ppm) = 156.11 (C2), 152.35 (C7), 139.45 (C1), 125.00 (C4/C6), 116.85 (C5), 115.93 (C3), 114.68 (C4/C6), 52.11 (Pyrr.), 48.70 (Pyrr.), 26.05 (Pyrr.), 24.95 (Pyrr.), -4.64 (Al$\underline{Me}$). Elemental Analysis: calcd for $C_{23}H_{29}AlN_4O_2$: C, 65.70; H, 6.95; N, 13.32. Found: C, 64.31; H, 7.44; N, 13.00.

Synthesis of 3b.

This compound was prepared similarly to **1b** using **L3H** ligand (254 mg, 1 mmol). Complex **2b** was isolated as a greenish powder (238 mg, 87% yield). NMR spectra show the signals of two isomers at 298 K in a 1/0.8 ratio (based on the integration of the two signals at 2.35 and 2.29 ppm) which tend to merge at 383 K. ^{1}H NMR (400 MHz, pyridine-d_5, 298 K): δ(ppm) = (*Aromatic signals of both isomers overlap)* 7.49-7.35 (overlapping signals, 4H, Ar.), 7.26-7.00 (overlapping signals, 12H, Ar.), 6.94-6.83 (overlapping signals, 8H, Ar.), 6.52-6.44 (overlapping signals, 4H, Ar.), 6.44-6.34 (overlapping signals, 4H, Ar.), 3.63 (broad signal, 12H, -N$\underline{Me}_2$), 2.82 (broad s, 12H, -N$\underline{Me}_2$), 2.35 (s, 6H, *o*-C$\underline{H}_3$), 2.29 (s, 6H, *o*-C$\underline{H}_3$), -0.17 (s overlapping with singlet at -0.18, 3H, Al$\underline{Me}$), -0.18 (s overlapping with singlet at -0.17, 3H, Al$\underline{Me}$). {^{1}H}^{13}C NMR (101 MHz, pyridine-d_5, 298 K): δ(ppm) = 169.29 (C^{IV}), 169.16 (C^{IV}), 157.67 (C^{IV}), 157.63 (C^{IV}), 140.04 (C^{IV}), 139.79 (C^{IV}), 138.53 (C^{IV}), 138.44 (C^{IV}), 134.36 (C^{IV}), 134.29 (C^{IV}), 131.45(CH), 131.40 (CH), 131.35 (CH), 131.07 (CH), 130.60 (2xCH), 126.71 (CH), 126.56 (CH), 124.74 (CH), 124.71 (CH), 123.06 (CH), 122.77 (CH), 116.68 (CH), 116.65 (CH), 116.57 (CH), 116.52 (CH), 41.93 (2xCH_3), 41.80 (2xCH_3), 40.28 (2xCH_3), 40.16 (2xCH_3), 19.79 (2xCH_3), 19.66 (2xCH_3), -5.87 (2xCH_3). ^{1}H NMR (400 MHz, pyridine-d_5, 383 K): δ(ppm) = 7.51-7.40 (broad signal, 2H, Ar.), 7.30-7.09 (broad overlapping signals, 6H, Ar.), 6.93-6.82 (broad signal, 4H, Ar.), 6.52-6.45 (m, 2H, Ar.), 6.45-6.36 (m, 2H, Ar.), 3.30 (broad s, 12H, N$\underline{Me}_2$), 2.42/2.37 (two s, 6H, *o*-C$\underline{H}_3$), -0.18 (broad s, 3H, Al$\underline{Me}$). Elemental Analysis: calcd for $C_{33}H_{37}AlN_4O_2$: C, 72.24; H, 6.80; N, 10.21. Found: C, 71.79; H, 7.27; N, 10.23.

Synthesis of 4b.

This compound was prepared similarly to **1b** using **L4H** ligand (280 mg, 1 mmol). Complex **2b** was isolated as a pale greenish powder (272 mg, 91% yield). NMR spectra show the signals of two isomers at 298 K in a 1/1 ratio (based on the integration of the two signals at 2.40 and 2.35 ppm). ^{1}H NMR (400 MHz, Pyridine-d_5 , 298 K*): δ(ppm) = (Aromatic signals of both isomers overlap),* 7.58-7.44 (overlapping signals, 4H, Ar.), 7.33-7.02 (overlapping signals, 12H, Ar.), 7.00-6.82 (overlapping signals, 8H, Ar.), 6.68-6.57 (overlapping signals, 4H, Ar.), 6.49-6.37 (overlapping signals, 4H, Ar.), 4.62-3.97 (overlapping signal, 8H, Pyrr.), 3.27 (broad signal, 4H, Pyrr.), 3.09 (broad signal, 4H, Pyrr.), 2.40 (s, 6H, *o*-C$\underline{H}_3$), 2.35 (s, 6H, *o*-C$\underline{H}_3$), 1.81 (broad signal, 16H, Pyrr.), -0.09 (broad overlapping signal, 3H, Al$\underline{Me}$), -0.11 (broad overlapping signal, 3H, Al$\underline{Me}$). {^{1}H}^{13}C NMR (101 MHz, Pyridine-d_5, 298 K): δ(ppm) = 166.11 (C^{IV}), 165.92 (C^{IV}), 157.66 (C^{IV}), 157.55 (C^{IV}), 140.08 (C^{IV}), 139.77 (C^{IV}), 137.63 (C^{IV}), 137.44 (C^{IV}), 135.37 (C^{IV}), 135.07 (C^{IV}), 131.65 (CH), 131.44 (CH), 131.11 (CH), 130.47 (CH), 130.25 (2xCH), 126.65 (CH), 126.32 (CH), 124.58 (CH), 124.55 (CH), 123.57 (CH), 123.08 (CH), 116.61 (CH), 116.53 (CH), 116.28 (CH), 116.23 (CH), 51.83 (2xCH_2), 51.76 (2xCH_2), 50.94 (2xCH_2), 50.64 (2xCH_2), 26.08 (4xCH_2), 25.97 (4xCH_2), 19.81(CH_3), 19.74 (CH_3), -5.40 (2xCH_3). Elemental Analysis: calcd for $C_{37}H_{41}AlN_4O_2$: C, 73.98; H, 6.88; N, 9.33. Found: C, 72.80; H, 7.15; N, 9.19.

Synthesis of 6b

This compound was prepared similarly to **1b** using **L6H** ligand (221 mg, 1 mmol). Complex **6b** was isolated as a whitish powder (220 mg, 70% yield). ^{1}H NMR (400 MHz, THF-d8, 298 K): δ(ppm) = 7.81 (s, 2H, H7), 6.79-6.69 (overlapping signals, 4H, H4 + H6), 6.53 (d, *J* = 7.7 Hz, 2H, H3), 6.43 (t, *J* = 7.5 Hz, 2H, H5), 3.56-3.37 (overlapping signals, 10H, H8 + H9), 2.68-2.47 (overlapping signals, 4H, H10), 2.26 (s, 12H, H11 + H12), -0.77 (s, 3H, Al<u>Me</u>). {^{1}H}^{13}C NMR (101 MHz, THF-d8, 298K): δ(ppm) = 157.07 (C7), 156.86(C2), 140.43 (C1), 124.76 (C4/C6), 116.29 (C5), 115.76 (C3), 115.51 (C4/C6), 58.39 (C10), 54.03 (C8/C9), 45.70 (C11+C12), 36.87 (C8/C9), -4.71 (Al<u>Me</u>). Elemental Analysis: calcd for $(C_{25}H_{39}AlN_6O_2)_{100}(C_2H_6OSi)_{15}$: C, 61.55; H, 8.15; N, 17.02. Found: C, 61.40; H, 8.18; N, 16.52.

Synthesis of 1b'.

In a glovebox, 147 mg (0.4 mmol) of **1b** were suspended in 4 mL of toluene. 30.6 µL of isopropanol (24.04 mg, 0.4 mmol, 1 equiv.) were then added with a microsyringe and the mixture was heated at 100 °C for 2 h. Cooling the solution to r.t. allowed the product to precipitate as a white solid which was filtrated and then dried under vacuum, affording **1b'** (100 mg, 61% yield). ^{1}H NMR (600 MHz, CD_2Cl_2, 298 K): δ(ppm) = 7.75 (s, 2H, H7), 6.90 (t, *J* = 7.2 Hz, 2H, H4), 6.85 (d, *J* = 7.8 Hz, 2H, H6), 6.68 (d, *J* = 7.6 Hz, 2H, H3), 6.62 (t, *J* = 7.6 Hz, 2H, H5), 3.93 (m, 1H, OC<u>H</u>(CH$_3$)$_2$), 3.44 (s (Δν$_{½}$ = 13.0 Hz), 6H, NMe$_2$), 3.24 (s (Δν$_{½}$ = 13.0 Hz), 6H, NMe$_2$), 0.98 (d, *J* = 5.8 Hz, 3H, OCH(C<u>H</u>$_3$)$_2$), 0.76 (d, *J* = 5.5 Hz, 3H, OCH(C<u>H</u>$_3$)$_2$). {^{1}H}^{13}C NMR (150 MHz, CD_2Cl_2, 298 K): δ(ppm) = 156.21 (C7), 155.60 (C2), 139.14 (C1), 125.12 (C4), 117.00 (C5), 115.49 (C3), 114.89 (C6), 63.28 (O<u>C</u>H(CH$_3$)$_2$), 43.49 (NMe$_2$), 38.59 (NMe$_2$), 27.57 (OCH(<u>C</u>H$_3$)$_2$), 27.39 (OCH(<u>C</u>H$_3$)$_2$). Elemental Analysis: calcd for $C_{21}H_{29}AlN_4O_3$: C, 61.15; H, 7.09; N, 13.58. Found: C, 61.16; H, 6.98; N, 13.41.

Synthesis of 1c.

In a glovebox, 133 mg (0.8 mmol) of **L1H** were solubilized in 5 mL of dried THF. 0.8 mL (0.8 mmol, 1 equiv.) of a 1 M solution of $ZnEt_2$ in hexane was added and the mixture was stirred at r.t. for 2 h. The volatiles were evaporated under vacuum and the solid obtained was washed with 4 mL of pentane before being dried under vacuum affording **1c** as a whitish powder (131 mg, 62% yield). ^{1}H NMR (400 MHz, pyridine-d$_5$, 298 K): δ(ppm) = 7.97 (s, 1H, H7), 7.34 (dd, *J* = 7.9, 1.5 Hz, 1H, H3), 7.23 (m, 1H, H4), 7.11 (dd, *J* = 7.7, 1.7 Hz, 1H, H6), 6.65 (td, *J* = 7.5, 1.6 Hz, 1H, H5), 2.93 (broad s (Δν$_{½}$ = 23.2 Hz), 6H, NMe$_2$), 1.62 (t, *J* = 8.1 Hz, 3H, ZnCH$_2$C<u>H</u>$_3$), 0.69 (q, *J* = 8.1 Hz, 2H, ZnC<u>H</u>$_2$CH$_3$). {^{1}H}^{13}C NMR (101 MHz, pyridine-d$_5$, 298 K): δ(ppm) = 164.38 (C2), 155.92 (C7), 139.20 (C1), 126.74 (C4), 118.63 (C3), 117.29 (C6), 113.39 (C5), 41.46 (extracted from HSQC, N<u>Me</u>$_2$), 36.74 (extracted from HSQC, N<u>Me</u>$_2$), 14.43 (ZnCH$_2$<u>C</u>H$_3$), 0.24 (Zn<u>C</u>H$_2$CH$_3$). Elemental Analysis: calcd for $C_{11}H_{16}ZnN_2O$: C, 51.28; H, 6.26; N, 10.87. Found: C, 50.03; H, 6.58; N, 10.38.

Synthesis of 2c.

This compound was prepared similarly to **1c** using **L2H** ligand (100 mg, 0.53 mmol). Complex **2c** was isolated as a whitish solid powder (114 mg, 76% yield). ^{1}H NMR (400 MHz, pyridine-d$_5$, 298 K): δ(ppm) = 8.26 (s, 1H, H7), 7.35 (dd, *J* = 7.9, 1.5 Hz, 1H, H3), 7.29-7.15 (m, 2H, H4 + H6), 6.67 (m, 1H, H5), 3.48 (broad (Δν$_{½}$ = 113.4 Hz), 4H, Pyrr.), 1.83-1.52 (overlapping signals, 7H, Pyrr. + ZnCH$_2$C<u>H</u>$_3$), 0.74 (q, *J* = 8.1 Hz, 2H, ZnC<u>H</u>$_2$CH$_3$). {^{1}H}^{13}C NMR (151 MHz, pyridine-d$_5$, 298 K): δ(ppm) = 164.55 (C2), 152.41 (C7), 139.04 (C1), 126.63 (C4/C6), 118.79 (C3), 116.70 (C4/C6), 113.28 (C5), 25.38 (Pyrr.), 14.52 (ZnCH$_2$<u>C</u>H$_3$), 0.42 (Zn<u>C</u>H$_2$CH$_3$). Elemental Analysis: calcd for $C_{13}H_{18}ZnN_2O$: C, 55.04; H, 6.40; N, 9.88. Found: C, 54.80; H, 6.10; N, 9.65.

Synthesis of 5c.

This compound was prepared similarly to **1c** using **L5H** ligand (316 mg, 1 mmol). Complex **5c** was isolated as a whitish solid powder (384 mg, 93% yield). ^{1}H NMR (500 MHz, pyridine-d$_5$, 298 K): δ(ppm) = 8.19 (d, *J* = 8.2 Hz, 1H, H3'), 7.86 (d, *J* = 8.1 Hz, 1H, H5'), 7.82 (d, *J* = 8.1 Hz, 1H, H8'), 7.59 (d, *J* = 7.1 Hz, 1H, H6'), 7.46 (d, *J* = 6.9 Hz, 2H, H4' + H10'), 7.27 (t, *J* = 7.5 Hz, 1H, H9'), 7.15 (d, *J* = 7.7 Hz, 1H, H6), 6.79 (t, *J* = 7.1 Hz, 1H, H4), 6.59 (d, *J* = 7.4 Hz, 1H, H3), 5.96 (t, *J* = 7.2 Hz, 1H, H5), 4.26-3.82 (m, 2H, Pyrr.), 3.07-2.67 (m, 2H, Pyrr.), 1.85-1.50 (overlapping signals, 7H, ZnCH$_2$C<u>H</u>$_3$ + Pyrr.), 0.82 (m, 2H, ZnC<u>H</u>$_2$CH$_3$). {^{1}H}^{13}C NMR (125 MHz, pyridine-d$_5$, 298 K): δ(ppm) = 163.85 (C2), 163.18 (C7), 138.33 (C1), 133.36 (C1'), 132.64 (C2'), 131.07 (C7'), 129.88 (C8'), 128.94 (C5'), 127.70 (C6'), 127.49 (C10'), 126.38 (C4'), 125.50 (C9'), 124.88 (C4), 124.68 (C3'), 121.76 (C3), 117.38 (C6), 111.81 (C5), 48.98 (Pyrr.), 25.06 (Pyrr.), 13.89 (ZnCH$_2$<u>C</u>H$_3$), -0.81 (ZnC<u>H</u>$_2$CH$_3$). Elemental Analysis: calcd for $C_{23}H_{24}ZnN_2O$: C, 67.41; H, 5.90; N, 6.84. Found: C, 65.62; H, 5.91; N, 6.62.

Synthesis of 6c.

In a glovebox, 221 mg (1 mmol, 1equiv.) of the corresponding amidine proligand was dissolved in 10 mL of dried THF. 1 mL (1 mmol, 1equiv.) of a 1M solution of $ZnEt_2$ in hexanes was then added and the resulting mixture was stirred at r.t for 2h. The solvent was then evaporated and the whitish powder was dried under vacuum (220 mg, yield 70%). ^{1}H NMR (500 MHz, TDF-d$_8$, 298 K): δ(ppm) = 7.88 (s, 1H, H7), 6.74 (overlapping signals, 3H, H4 + H6 + H3), 6.41 (broad singlet (Δν$_{½}$ = 25.8 Hz), 1H, H5), 3.43 (broad singlet (Δν$_{½}$ = 34.3 Hz), 2H, H9), 3.30 (broad singlet (Δν$_{½}$ = 28.3 Hz), 3H, H8), 2.46 (broad singlet (Δν$_{½}$ = 30.4 Hz), 2H, H10), 2.22 (s, 6H, H11 + H12), 0.92 (broad singlet (Δν$_{½}$ = 25.1 Hz), 3H, ZnCH$_2$C<u>H</u>$_3$), -0.09 (broad singlet (Δ$_{ν½}$ = 28.5 Hz), 2H, ZnC<u>H</u>$_2$CH$_3$). {^{1}H}^{13}C NMR (125 MHz, TDF-d$_8$, 298 K): δ(ppm) = 159.41 (C2), 156.06 (C7), 139.80 (C1), 124.98 (C3/C4/C6), 118.95 (C3/C4/C6), 116.90 (C3/C4/C6), 116.56 (C5), 58.47 (C10), 53.47 (C9), 45.75 (C11 + C12), 35.19 (C8), 13.03 (ZnCH$_2$<u>C</u>H$_3$), -0.32 (Zn<u>C</u>H$_2$CH$_3$). Elemental Analysis: calcd for $C_{14}H_{23}N_3OZn$: C, 53.43; H, 7.37; N, 13.35. Found: C, 53.00; H, 7.19; N, 12.87.

Synthesis of 1d.

In a glovebox, 354 mg (2.2 mmol) of **L1H** was dissolved in 10 mL of dried THF. 1.1 mL (1.1 mmol, 0.5 equiv.) of a 1M solution of $ZnEt_2$ in hexane was then added and the resulting mixture was

stirred at r.t. for 2 h. After having evaporated the solvents, the residue was washed with 6 mL of pentane and dried under vacuum affording **1d** as a whitish powder (343 mg, 80% yield). ^{1}H NMR (500 MHz, CD_2Cl_2, 298 K): δ(ppm) = 7.95 (s, 2H, H7), 6.90 (overlapping signals, 4H, Ar), 6.75 (d, *J* = 7.9 Hz, 2H, Ar), 6.46 (t, *J* = 7.5 Hz, 2H, Ar), 3.13 (s ($\Delta\nu_{½}$ = 7.6 Hz), 6H, N$\underline{Me}_2$), 2.91 (s ($\Delta\nu_{½}$ = 7.5 Hz), 6H, N$\underline{Me}_2$). {^{1}H}^{13}C NMR (125 MHz, CD_2Cl_2, 298 K): δ(ppm) (selected signals) = 155.31 (C7), 126.19 (Ar), 118.16 (Ar), 115.47 (Ar), 114.22 (Ar), 42.90 (CH_3, N$\underline{Me}_2$), 35.79 (CH_3, N$\underline{Me}_2$). Quaternary carbons not seen. Very few soluble, not enough for HMBC experiment. Elemental Analysis: calcd for $C_{18}H_{22}ZnN_4O_2$: C, 55.18; H, 5.66; N, 14.30. Found: C, 55.22; H, 5.97; N, 13.95.

Synthesis of 2d.

This compound was prepared similarly to **1d** using **L2H** ligand (380 mg, 2 mmol). Complex **2d** was isolated as a whitish solid powder (175 mg, 40% yield). ^{1}H NMR (500 MHz, CD_2Cl_2, 298 K): δ (ppm) = 8.23 (2H, s, H7), 6.95 (dd, *J* = 7.9, 1.6 Hz, 2H, H3), 6.90 (td, *J* = 7.6, 1.6 Hz, 2H, H4), 6.74 (dd, *J* = 8.0, 1.5 Hz, 2H, H6), 6.45 (td, *J* = 7.5, 1.5 Hz, 2H, H5), 3.62 (m, 4H, Pyrr.), 3.37 (m, 4H, Pyrr.), 1.84 (m, 4H, Pyrr.), 1.73 (m, 4H, Pyrr.). {^{1}H}^{13}C NMR (125 MHz, CD_2Cl_2, 298 K): δ (ppm) = 160.68 (C2), 151.43 (C7), 136.12 (C1), 125.87 (C4), 118.26 (C6), 114.66 (C3), 114.01 (C5), 51.52 (Pyrr.), 45.63 (Pyrr.), 25.35 (Pyrr.), 24.94 (Pyrr.).Elemental Analysis: calcd for $C_{22}H_{26}N_4O_2Zn$: C, 59.53; H, 5.90; N, 12.62. Found: C, 59.58; H, 5.35; N, 12.45.

Synthesis of 3d.

This compound was prepared similarly to **1d** using **L3H** ligand (254 mg, 1 mmol). Complex **3d** was isolated as a yellowish solid powder (133 mg, 46% yield). ^{1}H NMR (400 MHz, pyridine-d_5, 378 K): δ(ppm) = 7.52 (broad signal ($\Delta\nu_{½}$ = 18.2 Hz), 2H, Ar), 7.21 (m overlapping with residual Pyr. signals, 2H, Ar), 7.04 (m, 2H, Ar), 6.94 (t, *J* = 7.5 Hz, 2H, Ar), 6.58 (d, *J* = 7.6 Hz 2H, Ar), 6.35 (t, *J* = 7.3 Hz, 2H, Ar), 3.05 (broad signal ($\Delta\nu_{½}$ = 7.8 Hz), 12H, N$\underline{Me}_2$), 2.53 (broad signal overlapping with signal at 2.46, 3H, *o*-C$\underline{H}_3$), 2.46 (broad signal overlapping with signal at 2.53, 3H, *o*-C$\underline{H}_3$). {^{1}H}^{13}C NMR (101 MHz, pyridine-d_5, 378 K): δ(ppm) = 166.95, 161.73, 138.50, 137.98, 137.06, 129.92 (x2), 128.70, 125.09, 123.83, 122.16, 116.96, 112.20, 38.38, 18.90. Elemental Analysis: calcd for $C_{32}H_{34}N_4O_2Zn$: C, 67.19; H, 5.99; N, 9.79. Found: C, 66.55; H, 6.13; N, 9.68.

Synthesis of 4d.

This compound was prepared similarly to **1d** using **L4H** ligand (280 mg, 1 mmol). Complex **4d** was isolated as a yellowish solid powder (174 mg, 55% yield). ^{1}H NMR (400 MHz, pyridine-d_5, 383 K): δ(ppm) = 7.52 (broad ($\Delta\nu_{½}$ = 17.9 Hz), 2H), 7.30-7.11 (overlapping signals with residual Pyr, 6H), 7.07 (d, *J* = 7.6 Hz, 2H), 6.93 (t, *J* = 7.6 Hz, 2H), 6.66 (d, *J* = 6.6 Hz, 2H), 6.35 (m, 2H), 3.85-3.30 (m, 8H, Pyrr.), 2.49 (broad singlet, ($\Delta\nu_{½}$ = 14.8 Hz), 6H, o-CH_3), 1.80 (broad ($\Delta\nu_{½}$ = 13.7 Hz), 8H, Pyrr.). {^{1}H}^{13}C NMR (101 MHz, pyridine-d_5, 383 K): δ(ppm) = 164.48, 162.09, 137.43, 136.33, 130.53, 129.49, 129.12, 125.54, 124.42, 122.35, 117.25, 112.61, 48.73, 24.89, 19.10. One C not seen probably overlapping with other signals. Elemental Analysis: calcd for $C_{36}H_{38}N_4O_2Zn$: C, 69.28; H, 6.14; N, 8.98. Found: C, 69.25; H, 5.68; N, 9.32.

Synthesis of 5d.

This compound was prepared similarly to 1d using **L5H** ligand (316 mg, 1 mmol). Complex 5d was isolated as a yellowish solid powder (160 mg, 45% yield). ^{1}H NMR (400 MHz, pyridine-d5, 383 K): δ(ppm) = 8.52 (broad ($\Delta\nu_{½}$ = 57.0 Hz), 2H), 7.96-7.78 (overlapping signals, 6H), 7.70-7.59 (m, Pyr.-d_5 + 2H), 7.52 (t, *J* = 7.6 Hz, 2H), 7.43 (broad ($\Delta\nu_{½}$ = 24.0 Hz), 2H), 6.99 (d, *J* = 7.8 Hz, 2H), 6.81 (t, *J* = 7.6 Hz, 2H), 6.72 (d, *J* = 7.6 Hz, 2H), 6.13 (t, *J* = 7.4 Hz, 2H), 3.85-3.40 (m, 8H, Pyrr.), 1.81 (broad ($\Delta\nu_{½}$ = 16.7 Hz), 8H, Pyrr.). {^{1}H}^{13}C NMR (101 MHz, pyridine-d5, 383 K): δ(ppm) = 163.81, 162.05, 138.68, 133.66, 133.57, 131.49, 129.48, 128.59, 127.69, 127.30, 126.05, 125.28, 124.38, 121.78, 117.27, 112.51, 48.77 (CH_2, Pyrr.), 24.92 (CH_2, Pyrr.). One C not seen probably overlapping with other signals. Elemental Analysis: calcd for $C_{42}H_{38}ZnN_4O_2$: C, 72.46; H, 5.50; N, 8.05. Found: C, 72.16; H, 5.42; N, 8.25.

Synthesis of 6d.

This compound was prepared similarly to **1d** using **L6H** ligand (221.3 mg, 1 mmol). Complex **6d** was isolated as a whitish solid powder (151 mg, 60% yield).
^{1}H NMR (500 MHz, CD_2Cl_2, 298 K): δ (ppm) = 7.97 (2H, s, H7), 6.95-6.82 (overlapping signals, 4H, H4 + H6), 6.74 (d, *J* = 7.7 Hz, 2H, H3), 6.45 (t, *J* = 7.4, Hz, 2H, H5), 3.37 (broad signal, 4H, H9), 2.93 (s, 6H, H8), 2.41 (broad signal, 4H, H10), 2.21 (m, 12H, H11 + H12). {^{1}H}^{13}C NMR (125 MHz, CD_2Cl_2, 298 K): δ (ppm) = 160.82 (C2), 155.62 (C7), 136.57 (C1), 126.06 (C4/C6), 118.03 (C3), 115.60 (C4/C6), 114.11 (C5), 57.52 (C10), 53.62 (C9), 45.72 (C11 + C12), 34.27 (C8). Elemental Analysis: calcd for $(C_{24}H_{36}N_6O_2Zn)_{100}(C_2H_6SiO)_{30}$: C, 55.94; H, 7.21; N, 15.91. Found: C, 55.26; H, 7.14; N, 15.56.

Author Contributions

This project was conceived by JB, RMK and PLG. All experiments were performed by BT, VVC, CB, JB and RMK. X-ray diffraction studies were performed by YR. The manuscript was written by PLG. All authors have given approval to the final version of the manuscript.

Conflicts of interest

There are no conflicts to declare.

Acknowledgements

We thank Dr Quentin Bonnin and Ms Marie-José Penouilh-Suzette (PACSMUB) for technical assistance with NMR spectroscopy and MALDI-ToF analysis. Prof. Jean-Pierre Couvercelle and Mr Sylvain Quillard are warmly thanked for their assistance in GPC measurements. Financial support from Ministère de l'Enseignement Supérieur et de la Recherche, the Centre National de la Recherche Scientifique (CNRS), ANR (MORFAL, ANR-22-CE07-0011), are gratefully acknowledged.

Conseil Régional de Bourgogne Franche-Comté is acknowledged for financing the PhD grant of B.T. under the "Itinéraire Chercheurs Entrepreneurs" (ICE) program.

Notes and references

1 R. Hernández-Molina, A. Mederos, 1.19 - Acyclic and Macrocyclic Schiff Base Ligands. In *Comprehensive Coordination Chemistry II*, J. A. McCleverty, T. J., Meyer, Eds. Pergamon: Oxford, 2003; pp 411-446.

2 (a) K. C. Gupta and A. K. Sutar, *Coord. Chem. Rev.*, 2008, **252**, 1420. (b) H. Makio, H. Terao, A. Iwashita and T. Fujita, *Chem. Rev.*, 2011, **111**, 2363. (c) O. Santoro, X. Zhang and C. Redshaw, *Catalysts*, 2020, **10**, 800. (d) T. Aratani, *Pure Appl. Chem.*, 1985, **57**, 1839. (e) N. Kurono and T. Ohkuma, *ACS Catalysis*, 2016, **6**, 989. (f) F. Sha, B. S. Mitchell, C. Z. Ye, C. S. Abelson, E. W. Reinheimer, P. LeMagueres, J. D. Ferrara, M. K. Takase and A. R. Johnson, *Dalton Trans.*, 2019, **48**, 9603.

3 (a) H.-L. Yang, P. Cai, Q.-H. Liu, X.-L. Yang, S.-Q. Fang, Y.-W. Tang, C. Wang, X.-B. Wang and L.-Y. Kong, *Biorg. Med. Chem.*, 2017, **25**, 5917. (b) P. L. Zhang, X. X. Hou, M. R. Liu, F. P. Huang and X. Y. Qin, *Dalton Trans.*, 2020, **49**, 6043.

4 G. Peng, Y. Chen, B. Li, Y. Q. Zhang and X. M. Ren, *Dalton Trans.*, 2020, **49**, 5798.

5 (a) A. Ren, D. Zhu and Y. Luo, *J. Mol. Struct.*, 2020, **1209**, 127914. (b) P. Ghorai, K. Pal, P. Karmakar and A. Saha, *Dalton Trans.*, 2020, **49**, 4758-4773. (c) J. Sun, H. Yang, O. Simalou, K. Lv, L. Zhai, J. Zhao and R. Lu, *New J. Chem.*, 2019, **43**, 10134.

6 (a) X. Liu, W. Gao, Y. Mu, G. Li, L. Ye, H. Xia, Y. Ren and S. Feng, *Organometallics*, 2005, **24**, 1614. (b) D. Samuel, L. B. Franck, W. Richard, B.-L. Stéphane and M.-F. Aline, *Chem. Eur. J.*, 2007, **13**, 3202. (c) T. Cheisson, T.-P.-A. Cao, X. F. Le Goff, A. Auffrant, *Organometallics*, 2014, **33**, 6193. (d) M.-C. Chang, W.-Y. Lu, H.-Y. Chang, Y.-C. Lai, M. Y. Chiang, H.-Y. Chen and H.-Y. Chen, *Inorg. Chem.*, 2015, **54**, 11292. (e) G. Sarada, B. Sim, W. Cho, J. Yoon, Y.-S. Gal, J.-J. Kim and S.-H. Jin, *Dyes and Pigments*, 2016, **131**, 60. (f) M. Li, X. Shu, Z. Cai and M. S. Eisen, *Organometallics*, 2018, **37**, 1172. (g) A. W. Waltman and R. H. Grubbs, *Organometallics*, 2004, **23**, 3105. (h) C. Seok Oh, C. Won Lee and J. Yeob Lee, *Chem. Commun.*, 2013, **49**, 3875.

7 V. Vaillant-Coindard, B. Théron, G. Printz, F. Chotard, C. Balan, Y. Rousselin, P. Richard, I. Tolbatov, P. Fleurat-Lessard, E. Bodio, R. Malacea-Kabbara, J. Bayardon, S. Dagorne and P. Le Gendre, *Organometallics*, 2022, **41**, 2920.

8 F. Chotard, R. Lapenta, A. Bolley, A. Trommenschlager, C. Balan, J. Bayardon, R. Malacea-Kabbara, Q. Bonnin, E. Bodio, H. Cattey, P. Richard, S. Milione, A. Grassi, S. Dagorne, P. Le Gendre, *Organometallics*, 2019, **38**, 4147.

9 (a) C.-L. Lee, Y.-F. Lin, M.-T. Jiang, W.-Y. Lu, J. K. Vandavasi, L.-F. Wang, Y.-C. Lai, M. Y. Chiang and H.-Y. Chen, *Organometallics*, 2017, **36**, 1936. (b) F.-J. Lai, S.-J. Chung, Y.-L. Chang, Y.-T. Huang, C.-J. Chang, S. Ding, H.-Y. Chen, K.-H. Wu and Y.-F. Lin, *Eur. Polym. J.*, 2020, **135**, 109864.

10 FI ligands giving rise to 5-membered metallacycles have been used in olefin polymerization, see: (a) S. Yasuhiko, K. Norio and F. Terunori, *Chem. Lett.*, 2002, **31**, 358. (b) Y. Suzuki, H. Tanaka, T. Oshiki, K. Takai and T. Fujita, *Chem. Asian J.*, 2006, **1**, 878.

11 S. Kinoshita, K. Kawamura, T. Fujita, *Chem. Asian J.*, 2011, **6**, 284.

12 For reviews see: (a) C. A. Wheaton, P. G. Hayes and B. J. Ireland, *Dalton Trans.*, 2009, 4832. (b) T. Fuoco and D. Pappalardo, *Catalysts*, 2017, **7**, 64. (c) J. Gao, D. Zhu, W. Zhang, G. A. Solan, Y. Ma and W.-H. Sun, *Inorg. Chem. Front.*, 2019, **6**, 2619. For selected examples see: (d) M. H. Chisholm, J. C. Gallucci, H. Zhen and J. C. Huffman, *Inorg. Chem.*, 2001, **40**, 5051. (e) Z.-R. Dai, C.-F. Yin, C. Wang and J.-C. Wu, *Chin. Chem. Lett.*, 2016, **27**, 1649. (f) J. Payne, P. McKeown, M. F. Mahon, E. A. C. Emanuelsson and M. D. Jones, *Polym. Chem.*, 2020, **11**, 2381. (g) M. Fuchs, S. Schmitz, P. M. Schäfer, T. Secker, A. Metz, A. N. Ksiazkiewicz, A. Pich, P. Kögerler, K. Y. Monakhov and S. Herres-Pawlis, *Eur. Polym. J.*, 2020, **122**, 109302. (h) N. Iwasa, M. Fujiki and K. Nomura, *J. Mol. Catal. A: Chem.*, 2008, **292**, 67. (i) D. Pappalardo, L. Annunziata and C. Pellecchia, *Macromolecules*, 2009, **42**, 6056. (j) W. Zhang, Y. Wang, W.-H. Sun, L. Wang and C. Redshaw, *Dalton Trans.*, 2012, **41**, 11587. (k) M. Normand, V. Dorcet, E. Kirillov and J.-F. Carpentier, *Organometallics*, 2013, **32**, 1694. (l) Y. Jiang, W. Zhang, M. Han, X. Wang, G. A. Solan, R. Wang, Y. Ma and W.-H. Sun, *Polymer*, 2022, **242**, 124602.

13 (a) H. Bredereck, F. Effenberger and A. Hofmann, *Chem. Ber.*, 1964, **97**, 61. (b) E. D. Raczyńska, *J. Chem. Research, (S)*, 1987, 410.

14 J. Joseph, J. Y. Kim and S. Chang, *Chem. Eur. J.*, 2011, **17**, 8294.

15 D. J. Darensbourg, W. Choi, C. P. Richers, *Macromolecules*, 2007, **40**, 3521.

16 J. B. L. Gallaway, J. R. K. McRae, A. Decken and M. P. Shaver, *Can. J. Chem.*, 2012, **90**, 419.

17 (a) H.-Y. Chen, H.-Y. Tang and C.-C. Lin, *Macromolecules*, 2006, **39**, 3745. (b) W.-C. Hung, Y. Huang and C.-C. Lin, *J. Polym. Sci., Part A: Polym. Chem.*, 2008, **46**, 6466. (c) W.-C. Hung and C.-C. Lin, *Inorg. Chem.*, 2009, **48**, 728.

18 T. Ebrahimi, E. Mamleeva, I. Yu, S. G. Hatzikiriakos and P. Mehrkhodavandi, *Inorg. Chem.*, 2016, **55**, 9445.

19 (a) P. McKeown, S. N. McCormick, M. F. Mahon and M. D. Jones, *Polym. Chem.*, 2018, **9**, 5339.

20 F. Santulli, M. Lamberti, M. Mazzeo, *ChemSusChem* 2021, **14**, 5470. (b) S. D'Aniello, S. Laviéville, F. Santulli, M. Simon, M. Sellitto, C. Tedesco, C. M. Thomas, M. Mazzeo, *Catal. Sci. Technol.* 2022, **12**, 6142. (c) F. Santulli, G. Gravina, M. Lamberti, C. Tedesco, M. Mazzeo, *Mol. Catal.* 2022, **528**, 112480.

21 M. P. Coles, *Dalton Trans.*, 2006, 985.

22 I. D. Cunningham, J. Llor and L. Muñoz, *J. Chem. Soc., Perkin Trans. 2*, 1991, 1751.

23 A. W. Addison, T. N. Rao, J. Reedijk, J. van Rijn and G. C. Verschoor, *J. Chem. Soc., Dalton Trans.*, 1984, 1349.

24 M. Pinsky and D. Avnir, *Inorg. Chem.*, 1998, **37**, 5575.

25 F. M. García-Valle, V. Tabernero, T. Cuenca, M. E. G. Mosquera, J. Cano and S. Milione, *Organometallics*, 2018, **37**, 837.

26 A. Okuniewski, D. Rosiak, J. Chojnacki and B. Becker, *Polyhedron*, 2015, **90**, 47.

27 F.-J. Lai, L.-L. Chiu, C.-L. Lee, W.-Y. Lu, Y.-C. Lai, S. Ding, H.-Y. Chen and K.-H. Wu, *Polymer*, 2019, **182**, 121812.

28 R. Lal De, M. Mandal, L. Roy, J. Mukherjee, *Indian J. Chem.*, 2008, 47A, 207.